OPTIMIZATION OF ABRASIVE MACHINING OF DUCTILE CAST IRON USING WATER BASED SiO_2 NANOCOOLANT: A RADIAL BASIS FUNCTION

AZMA SALWANI BT. AB AZIZ

Report submitted in partial fulfillment of the requirements
for the award of
Bachelor of Mechanical Engineering

Faculty of Mechanical Engineering
UNIVERSITI MALAYSIA PAHANG

JUNE 2012

UNIVERSITI MALAYSIA PAHANG

BORANG PENGESAHAN STATUS TESIS

JUDUL: OPTIMIZATION OF ABRASIVE MACHINING OF DUCTILE CAST IRON USING WATER BASED SiO_2 NANOCOOLANT: A RADIAL BASIS FUNCTION

SESI PENGAJIAN: 2011/2012

Saya **AZMA SALWANI BT AB AZIZ (890115-06-5136)**
(HURUF BESAR)
mengaku membenarkan tesis (Sarjana Muda / ~~Sarjana / Doktor Falsafah~~)* ini disimpan di perpustakaan dengan syarat-syarat kegunaan seperti berikut:

1. Tesis ini adalah hakmilik Universiti Malaysia Pahang (UMP).
2. Perpustakaan dibenarkan membuat salinan untuk tujuan pengajian sahaja.
3. Perpustakaan dibenarkan membuat salinan tesis ini sebagai bahan pertukaran antara institusi pengajian tinggi.
4. **Sila tandakan (√)

☐	**SULIT**	(Mengandungi maklumat yang berdarjah keselamatan atau kepentingan Malaysia seperti yang termaktub di dalam AKTA RAHSIA RASMI 1972)
☐	**TERHAD**	(Mengandungi maklumat TERHAD yang telah ditentukan oleh organisasi / badan di mana penyelidikan dijalankan)
√	**TIDAK TERHAD**	

Disahkan oleh:

_____
(TANDATANGAN PENULIS)

Alamat Tetap:

Lot PT 471, Belakang Perumahan,
Taman Bunga Raya,
16210, Tumpat Kelantan.

Tarikh: **24 JUNE 2012**

_____
(TANDATANGAN PENYELIA)

Nama Penyelia:

Assoc. Prof. Dr. Md. Mustafizur Rahman

Tarikh: **24 JUNE 2012**

CATATAN: * Potong yang tidak berkenaan.

** Jika tesis ini SULIT atau TERHAD, sila lampirkan surat daripada pihak berkuasa/organisasi berkenaan dengan menyatakan sekali tempoh tesis ini perlu dikelaskan sebagai SULIT atau TERHAD.

◆ Tesis dimaksudkan sebagai tesis bagi Ijazah Doktor Falsafah dan Sarjana secara Penyelidikan, atau disertasi bagi pengajian secara kerja kursus dan penyelidikan, atau Laporan Projek Sarjana Muda (PSM).

UNIVERSITI MALAYSIA PAHANG
FACULTY OF MECHANICAL ENGINEERING

I certify that the project entitled "Optimization of Abrasive Machining of Ductile Cast Iron Using Water-Based Sio_2 Nanocoolant: A Radial Basis Function" is written by Azma Salwani Bt. Ab Aziz. I have examined the final copy of this project and in my opinion; it is fully adequate in terms of scope and quality for the award of the degree of Bachelor of Engineering. I herewith recommend that it be accepted in partial fulfillment of the requirements for the degree of Bachelor of Mechanical Engineering.

(DR. GIGIH PRIYANDOKO)
Examiner Signature

SUPERVISOR'S DECLARATION

I hereby declare that I have checked this project report and in my opinion this project is adequate in terms of scope and quality for the award of the degree of Bachelor of Mechanical Engineering.

Signature :
Name of Supervisor : DR. MD. MUSTAFIZUR RAHMAN
Position : ASSOCIATE PROFESSOR
Date : 24th JUNE 2012

STUDENT'S DECLARATION

I hereby declare that the work in this report is my own except for quotations and summaries which have been acknowledged. The report has not been accepted for any degree and is not concurrently submitted for award of other degree.

Signature :
Name : AZMA SALWANI BT. AB AZIZ
ID Number : MA08033
Date :

Special thanks to my parents and my late brother who always believe and support me.

Ab. Aziz Bin Ab. Rahman

Che Sabariah Bt Yahya

Azrul Shazlie Bin Ab. Aziz

ACKNOWLEDGEMENTS

First of all, I would like to thank to Allah S.W.T for giving me chance and strength to finish my Final Year Project in order to fulfill my Bachelor of Mechanical Engineering conditions. I also want to express my sincere appreciation to my supervisor, Assoc. Prof. Dr. Md. Mustafizur Rahman for his germinal ideas, invaluable guidance, continuous encouragement and constant support in order to complete this thesis. Without his guidance, I would not be able to finish this thesis completely. I am also would like to express my very special thanks to Mr. Aziha, lab instructor who guide me to handle the grinding machine and Mr. Azmi, lecturer who helped me in order to prepare the nanocoolant and also for his suggestion and co-operation throughout the study. I also sincerely thanks for the time spent proofreading and correcting my mistakes.

My sincere thanks go to all of my lab mates and members of the staff of Mechanical Engineering Department, Universiti Malaysia Pahang (UMP), who helped me in many ways during this thesis writing. I acknowledge my sincere indebtedness and gratitude to my parents for their love, dream and sacrifice throughout my life. Without your support I felt that there is no inspiration for me to keep moving in my journey of life. I am also indebted to all my friends and anyone who helped me during my completion of this thesis.

ABSTRACT

This report presents optimization of abrasives machining of ductile cast iron using water based SiO_2 nanocoolant. Conventional and nanocoolant grinding was peerformed using the precision surface grinding machine. Study was made to invetigate the effect of table speed and depth of cut towards the surface roughness and MRR. The best output parameters between conventional and SiO_2 nanocoolant are carry out at the end of the experiment. Mathematical modeling is developed using the response surface method. Artificial neural network (ANN) model is developed for predicting the results of the surface roughness and MRR. Multi-Layer Perception (MLP) along with batch back propagation algorithm are used. MLP is a gradient descent technique to minimize the error through a particular training pattern in which it adjusts the weight by a small amount at a time. From the experiment, depth of cut is directly proportional with the surface roughness but for the table speed, it is inversely proportional to the surface roughness. For the MRR, the higher the value of depth of cut, the lower the value of MRR and for the table speed is vice versa. As the conclusion, the optimize value for each parameters are obtain where the value of surface roughness and MRR itself was 0.174 μm and 0.101cm^3/s for the conventional- single pass, 0.186 μm and 0.010 cm^3/s for SiO_2- single pass, 0.191μm and 0.115cm^3/s for conventional-multiple pass, and 0.240μm and 0.112 cm^3/s for the SiO_2- multiple pass.

ABSTRAK

Laporan ini membincangkan tentang pengoptimuman pemesinan pelelas besi tuang mulur menggunakan SiO_2 nanopartikel. Kajian telah dibuat keatas kesan kelajuan meja dan kedalaman pemotongan terhadap kekasaran permukaan dan kadar penyingkiran bahan. Parameter output terbaik antara konvensional dan SiO_2 nanopartikel diperolehi pada akhir eksperimen. Pemodelan matematik dibangunkan dengan menggunakan kaedah respons permukaan. Model rangkaian neural tiruan dibangunkan untuk meramalkan keputusan kekasaran permukaan dan kadar penyingkiran bahan. Persepsi pelbagai lapisan bersama-sama dengan kelompok algoritma perambatan belakang digunakan. Persepsi pelbagai lapisan adalah teknik untuk mendapatkan kecerunan untuk meminimumkan kesilapan melalui corak latihan tertentu di mana ia menyesuaikan berat oleh jumlah kecil pada satu-satu masa. Daripada ujikaji tersebut, kedalaman pemotongan adalah berkadar langsung dengan kekasaran permukaan tetapi untuk kelajuan jadual, ia adalah berkadar songsang dengan kekasaran permukaan. Untuk kadar penyingkiran bahan, semakin tinggi nilai kedalaman pemotongan, lebih rendah nilai kadar penyingkiran bahan dan untuk kelajuan jadual adalah sebaliknya. Sebagai kesimpulan, mengoptimumkan nilai bagi setiap parameter adalah mendapatkan di mana nilai kekasaran permukaan dan MRR sendiri adalah 0,174 μm dan 0.101cm^3 / s untuk pas konvensional-tunggal, 0,186 μm dan 0,010 cm^3 / s untuk pas SiO_2-tunggal, 0,191 μm dan 0.115cm^3 / s pas konvensional berganda, dan 0.240μm dan 0,112 cm^3 / s untuk pas SiO_2-pelbagai.

TABLE OF CONTENTS

		Page
SUPERVISOR'S DECLARATION		ii
STUDENT'S DECLARATION		iii
DEDICATION		iv
ACKNOWLEDGEMENTS		v
ABSTRACT		vi
ABSTRAK		vii
TABLE OF CONTENTS		viii
LIST OF TABLES		xi
LIST OF FIGURES		xiii
LIST OF ABBREVIATIONS		xv
LIST OF SYMBOLS		xvi
CHAPTER 1	**INTRODUCTION**	
1.1	Background	1
1.2	Problem Statement	3
1.3	Project Objectives	3
1.4	Project Scopes	4
1.5	Organization of Report	4
CHAPTER 2	**LITERATURE REVIEW**	
2.1	Introduction	5
2.2	Types of Grinding	6
2.3	Thermal Analysis	9
2.4	Grinding Parameters	10
2.5	Selection of the Grinding Wheel	11
	2.5.1 Grinding wheel	11
	2.5.2 Grain density	12
	2.5.3 Aluminium oxide grinding wheel	12
	2.5.4 Silicon carbide grinding wheel	12

2.6	Selection of Cutting Fluid	13
	2.6.1 Cooling effect	13
	2.6.2 Lubrication effect	13
	2.6.3 Taking away formed chip from the cutting zone	14
2.7	Nanofluids	14
2.8	Preparation Method for Nanofluids	14
	2.8.1 Two-steps method	15
	2.8.2 One-step method	15
2.9	Response Surface Method	15
2.10	Artificial Neural Network	16
2.11	Radial Basis Function	16

CHAPTER 3 METHODOLOGY

3.1	Introduction	18
3.2	Workpiece Preparation	18
3.3	Experiment Details	22
3.4	Water based SiO2 Nanocoolant Preparation	25
3.5	Surface Roughness Tester	27
3.6	Scanning Electron Microscope	27
3.7	Design of Experiment	29
3.8	Response Surface Methodology	29
3.9	Artificial Neural Network	30
3.10	Data Analysis	33

CHAPTER 4 RESULTS AND DISCUSSION

4.1	Introduction	35
4.2	Mathematical Modeling	36
	4.2.1 First-order modeling	36
	4.2.2 Second-order modeling	39
4.3	Artificial Neural Network Analysis	43
4.4	Optimization	51
4.5	Microstructure Analysis	51

CHAPTER 5 CONCLUSION AND RECOMMENDATIONS

5.1 Conclusions 53

5.2 Recommendations 54

REFERENCES 55

LIST OF TABLES

Table No.	Title	Page
3.1	Properties of the SiO_2 nanoparticles	26
3.2	Design of Experiment	29
3.3	Experimental values and coded levels of the independent variables	30
3.4	Experimental results for conventional-Single pass	33
3.5	Experimental results for Silicon Oxide nanocoolant-Single pass	33
3.6	Experimental results for conventional-Multiple pass	34
3.7	Experimental results for Silicon Oxide nanocoolant- Multiple pass	34
4.1	ANOVA results for conventional coolant grinding	37
4.2	ANOVA results for SiO_2 nanocoolant grinding	37
4.3	ANOVA Results of second-order model for conventional grinding	40
4.4	ANOVA Results of second-order model for SiO_2 nanocoolant	40
4.5	Architecture search for conventional-Single Pass	43
4.6	Architecture search for SiO_2-Single Pass	44
4.7	The range of input and output parameters values for single pass grinding	47
4.8	The range of input and output parameters values for multiple pass grinding	47
4.9	Architecture search for conventional with multiple pass grinding	48
4.10	Architecture search for SiO_2 nanocoolant with multiple pass grinding	48

4.11	Comparison between RSM model and ANN for conventional coolant	51
4.12	Comparison between RSM model and ANN for silicon oxide nanocoolant	52

LIST OF FIGURES

Figure No.	Title	Page
2.1	Centerless Grinding	6
2.2	Surface Grinding	8
2.3	Centered grinding	9
3.1	Disc Cutter	19
3.2	Squaring using the milling machine	20
3.3	Milling Machine (PARTHNER)	20
3.4	Operations of the band saw cutting the workpiece	21
3.5	Band saw machine (EVERISING S-300HB)	21
3.6	Precision Surface Grinding Machine (STP-1022ADCII)	22
3.7	Tachometer	23
3.8	Infra-red thermometer	23
3.9	Silicon carbide grinding wheel	24
3.10	Water Based-Coolant	25
3.11	SiO_2 nanocoolant preparation	26
3.12	Surface roughness tester	27
3.13	Scanning electron machine	28
3.14	The architecture of developed ANN model	32
4.1	(a): Conventional-Single pass, (b): SiO_2-Single pass, (c): Conventional-Multiple pass, (d): SiO_2-Multiple pass	38
4.2	Contour plot for first order RSM model	39
4.3	(a): Conventional-Single pass, (b): SiO_2-Single pass, (c): Conventional-Multiple pass, (d): SiO_2-Multiple pass	41
4.4	Contour plot for second order RSM model	42

4.5	Actual versus predicted values for conventional-single pass	45
4.6	Actual versus predicted values for SiO_2-single pass	46
4.7	Actual versus predicted values for conventional-Multiple Pass	49
4.8	Actual versus predicted values for SiO_2-Multiple Pass	50
4.9	Microstructure of surface workpiece of conventional and nanocoolant grinding	52

LIST OF ABBREVIATIONS

MRR	Material Removal Rate
RSM	Response Surface Methodology
UMP	Universiti Malaysia Pahang
ANN	Artificial Neural Network
RBF	Radial Basis Function
SiO_2	Silicon Dioxide
h	Centre height
f_d	Longitudinal dressing feed-rate
n_r	Control wheel speed
v_{fa}	In-feed speed
R_a	Mean roughness
Al_2O_3	Aluminium Oxide
SiC	Silicon Carbide
SEM	Scanning Electron Microscope
ANOVA	Analysis of Variance
DOE	Design of Experiment
FKM	Fakulti Kejuruteraan Mekanikal
CCD	Central Composite Design
Eq.	Equation
MLP	Multi-Layer Perception
BP	Back Propagation

LIST OF SYMBOLS

y	Predicted response
β_0	Interception coefficient
β_1	Linear terms
β_2	Quadratic terms
ε	Interactions and the coded levels of the independent variables
X_1	Independent variable
X_2	Independent variable

CHAPTER 1

INTRODUCTION

1.1 BACKGROUND

Grinding is a manufacturing process with unsteady process behavior, whose complex characteristic determine the technological output and quality (Krajnik et al., 2005). Grinding is actually a finishing process used to improve surface finish, abrade hard materials, and tighten the tolerance on flat and cylindrical surface by removing a small amount of material. In grinding, an abrasive material rubs against the metal part and removes tiny pieces of material. The abrasive material is typically on the surface of wheel and abrades material in a way similar to sanding. On a microscopic scale, the chip formation in grinding is the same as that found in other machining process. The abrasive action of grinding generates excessive heat so that flooding of the cutting area with fluid is necessary. The selection of appropriate base fluid is very critical in the application of nanoparticles based lubricants in grinding. Grinding may be performed on a surface grinding machine which feeds the workpiece into the cutting tool. A cylindrical grinding machine which rotates the workpiece as the cutting tool feeds into it. Amount of material removal rate (MRR) are depend largely on the amount of the machine current and the spark on time in the cutting process (Newman and Ho, 2004). The speed of the material removal rate is specified on the rate the material that has being removed. The MRR are influenced by the melting temperature of the workpiece, the lower melting temperature will gave faster MRR (Helmi et al., 2010). The quality of machined surface is characterized by the accuracy of its manufacture with respect to the dimension specified by the designer. Every machining operation leaves characteristic evidence on the machined surface. This evidenced in form of finely spaced micro irregularities left by the cutting tool. Each type of cutting tool leaves its own individual

pattern which therefore can be identified. This pattern is known as surface roughness. Surface roughness is one of the most important factors for evaluating workpiece quality during the finishing process because the quality of surface affects the functional characteristics of the workpiece such as fatigue and fracture resistance and surface friction (Samhouri and Surgenor, 2005).

Nanofluids have the potential to be the next generation of coolants due to their significantly higher thermal conductivities. Nanofluids are formed by dispersing nanoparticles in base fluids such as water. It has been reported that the thermal conductivities of nanofluids increase dramatically due to the high thermal conductivity of solid particles suspended in the heat transfer fluid (Ding et al., 2009). Nanofluids/nanoparticles are particles that have one dimension that is 100 nanometers or less in size. The properties of many conventional materials change when formed from nanoparticles. This is typically because nanoparticles have a greater surface area per weight than larger particles; this causes them to be more reactive to certain other molecules. Nanoparticles are used, or being evaluated for use in many fields especially in medication and engineering fields.

The machining process is very complex, thus experimental and analytical models that are developed by using conventional approaches such as the statistical regression technique which is combined with the Response surface methodology (RSM) have remained as an alternative in the modeling of the machining process. RSM is practical, economical and relatively easy for used. The experimental data was utilized to build mathematical model for first-and-second order model by regression method. Bradley (2007) stated that when the response can be defined by a linear function of independent variables, then the approximating function is a first order model.

An artificial neural network is a system based on the operation of biological neural networks, in other words, is an emulation of biological neural system. Artificial neural network would be implementation necessary because although computing nowadays is truly advanced, there are certain tasks that a program made for a common microprocessor is unable to perform. Artificial neural network (ANN) has been developed as generalizations of mathematical models of biological nervous systems

(Abraham, 2005). A first wave of interest in neural networks also known as connectionist models or parallel distributed processing emerged after the introduction of simplified neurons by McCulloch and Pitts (1943).

1.2 PROBLEM STATEMENT

The environmental issues in machining industry concern mostly the cutting fluids. Coolants are widely used in machining processes to cool the tool and workpiece and to help remove chips from the cutting zone. Despite these benefits, the use of cutting fluids can present potential environmental problems. Coolants also cause harmful effects for the machine operator, as well as in disposal hazardous waste. In addition to the base oil, cutting fluids contain many kinds of additives such as emulsifiers, antioxidants, bactericides, tensides, EP-additives, corrosion inhibitors, agents for preventing foaming and etc. Although the cutting fluids are gradually being developed to be safer for the users and environment, they still have many disadvantages and risks that cannot be eliminated. Cutting fluids are entrained by chips and workpieces, and on the other hand, they contaminated machine tools, floor and workers. The SiO_2 nanoparticle as a coolant is used in this project.

1.3 PROJECT OBJECTIVES

The objectives of this project are as follows:

(i) To investigate the experimental performance of grinding of ductile cast iron based on response surface method.
(ii) To develop optimization model for grinding parameters using a Radial Basis Function (RBF) technique, and
(iii) To investigate the effect of water based SiO_2 nanoparticles to the precision surface grinding.

1.4 PROJECT SCOPES

The scopes of this project are to prepare the Design of Experiment, preparation of the SiO_2 nanocoolant. The experiment on grinding machine utilizing abrasive grinding wheel have to perform using water based SiO_2 of ductile cast iron. The performance will be carried out and also the material removal rate and surface roughness analysis. Statistical analysis using central composite method also will be done. The investigation of the effect of SiO_2 nanoparticles and conventional cooling fluid are using ANN.

1.5 ORGANIZATION OF REPORT

Chapter 2 presents the literature review that focused on recent studies by the previous researcher about the topic which is the effect of grinding process parameters on surface roughness of the ductile cast iron by using SiO_2 nanoparticles as a coolant. Chapter 3 will be discussed about the methodology that will conduct for this project such as the design of experiment, experiment setup, selection of parameters. Chapter 4 is about the analysis the results of surface roughness that obtained from the experiment due to the parameters selected. Chapter 5 will be summarized the overall finding and recommendation for future work.

CHAPTER 2

LITERATURE REVIEW

2.1 INTRODUCTION

Grinding is the most common form of abrasive machining. It is a material cutting process which engages an abrasive tool whose cutting elements are grains of abrasive material known as grit. These grits are characterized by sharp cutting points, high hot hardness, and chemical stability and wear resistance. The grits are held together by a suitable bonding material to give shape of an abrasive tool. Grinding may be classified in to groups as rough or non-precision grinding and precision grinding. Snagging and offhand grinding are the common forms of the rough grinding where the metal is removed without regard to accuracy. In precision grinding, according to type of surface to be ground, it is classified in to external or internal grinding, surface and cylindrical grinding (Malkin, 1984).

Material removal in grinding occurs by the interaction of abrasive grains in the grinding wheel with the workpiece at extremely high speeds and shallow penetration depths (Malkin, 1984). Therefore some practical methods are described for optimization of the grinding and dressing parameters by combining the grinding energy model and thermal analysis together with empirical relationships for surface finish and the influence of dressing parameters on grinding performance. For grinding of steels with aluminium oxide abrasive, it has been postulated that the controlling chemical reaction is the formation of a spindle between the oxidized metal and the aluminium oxide, which act as a transition layer for adhesion. In this case, lubrication effectiveness of grinding fluids might be attributed in part to their ability to reduce metal adhesion by inhibity spindle formation and also the sticking of metal chips to each other.

2.2 TYPES OF GRINDING

Grinding machines were originally used almost exclusively for truing tools steel parts, which were distorted by hardening. The great improvements have been made both in grinding machines and abrasive wheels, however, result from the application of the grinding process to the finishing of many unhardened parts. There are various types of grinding including the centerless grinding, cylindrical grinding, surface grinding, centered grinding and contour grinding.

Centerless Grinding: Centerless grinding is an abrasive machining process by which small chips of material are removed from the external surface of a cylindrical metallic or nonmetallic workpiece. This process relies on the relative rotations of the grinding wheel and regulating wheel to rotate the workpiece. The process does not require chucking or locating the workpiece between centers for rotation (Todd et al., 1994). Characteristic of this process requires no chucking or mounting of the workpiece. The centerless grinding also produces close tolerances and smooth surfaces. This process is applicable for cylindrical, stepped, formed and crucial workpiece. As other types of grinding, centerless grinding also requires coolant and is a primarily a finishing process (see Figure 2.1).

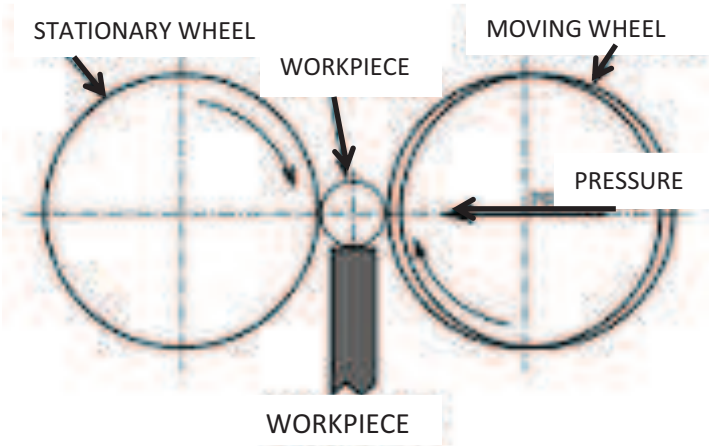

Figure 2.1: Centerless Grinding

Cylindrical Grinding: Cylindrical grinding is an abrasive machining process in which material is removed from the external surface of a metallic or nonmetallic cylindrical

workpiece by rotating the grinding wheel and workpiece in opposite directions while they are in contact with one another. The workpiece is mounted between centers and is rotated by means of a workpiece holder (Todd et al., 1994). The characteristic of this process is to produce straight tapered and formed workpiece. It is only used for cylindrical workpiece. Cylindrical grinding produces highly accurate surfaces and smooth finishes and also primarily a final machining process.

Surface Grinding: Surface grinders are machine tools used to provide precision regarding the level, size or finish of the surfaces. The longitudinal feed is usually powered by hydraulics or cross feed, and any mixture of hand, electrical or hydraulics operation styles may be used depending on the ultimate usage of the machine. There are a few types of surface grinding which are horizontal-spindle, vertical-spindle, vertical-spindle rotary grinding, horizontal spindle single disk, and vertical swivel head grinding. Figure 2.2 shows the various types of cylindrical grinding (source: Efunda Global).

Centered Grinding: Grinding for surfaces of rotation (axially symmetric surfaces) can be either centered or centerless. Centered grinding involves fixturing the part on a spindle axis as it is ground as Figure 2.3 (source: Efunda Global). This configuration can be compared to fixturing a part on a lathe with or without a tail stock. The abrasive material is on a grinding wheel that rotates in a direction such that rolling or sliding contact occurs where the wheel and workpiece touch. Centered grinding is accurate and stable, but setup takes time and through put surface.

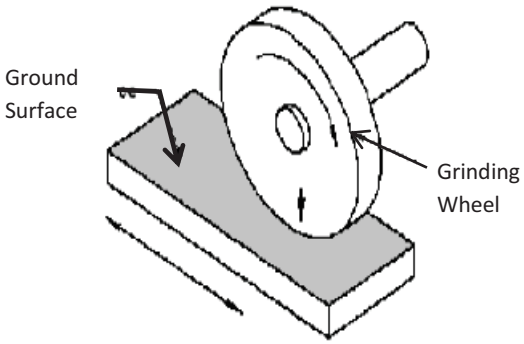

Horizontal-spindle reciprocating table surface grinding

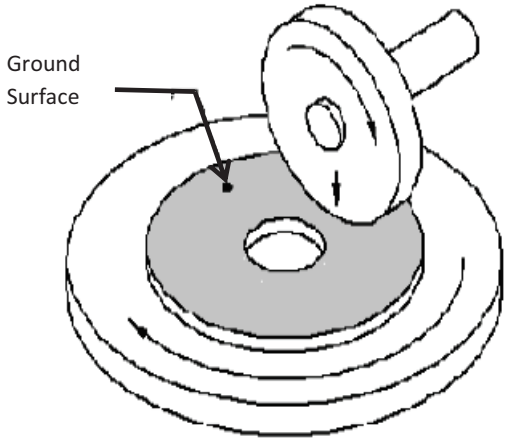

Horizontal-spindle rotary table surface grinding

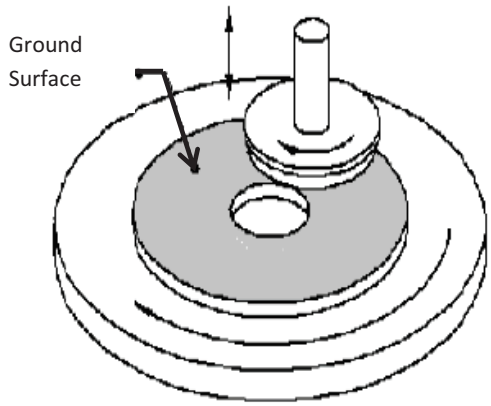

Vertical-spindle rotary table surface grinding

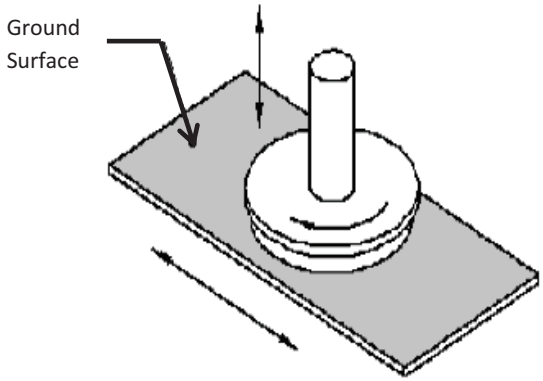

Vertical-spindle reciprocating table surface grinding

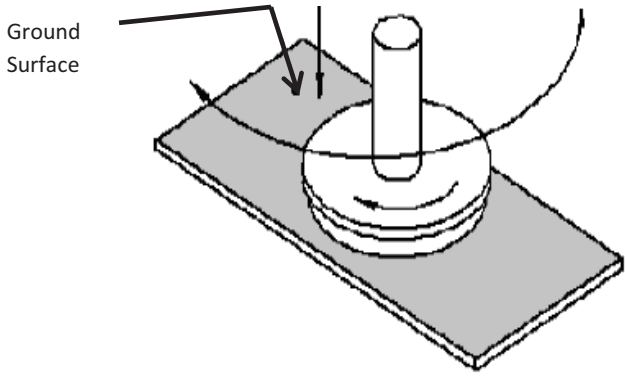

Figure 2.2: Surface Grinding

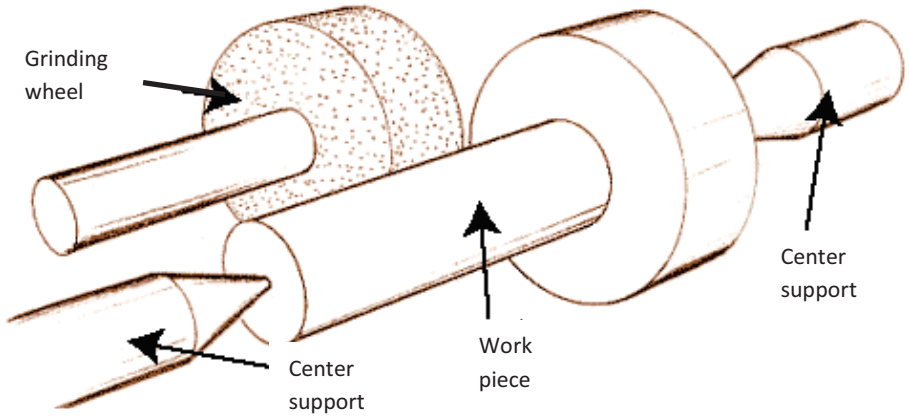

Figure 2.3: Centered grinding

2.3 THERMAL ANALYSIS

A thermal model of the wet grinding process has been used to predict the temperature at the workpiece surface. The model considers that the heat sources during grinding are from the abrasive grain workpiece interface and the shear plane between the workpiece and chip. During grinding, the power and energy is transmitted as well as heat is generated in the contact zone of the workpiece and grinding wheel. The sliding/friction may raise variety of modes of metal removal, including the plastic grooving which is relatively affect surface roughness. It is sensitive to material properties such as hardness, fatigue strength, toughness the operative values of which being dependent upon the strain, strain rate, and temperature generated in the contact zone. An excessive heat generates affect to the surface roughness (Kalpakjian and Schmid, 2001). In the metal working industry, the grinding process is a very important method of producing a precision part. For ductile materials, the specific energy generated during a grinding process is generally very high, and is mostly dissipated as heat in the wheel-workpiece contact (Liao et al., 1998). The removal rates can be achieved in grinding by the temperature generated. The grinding process required a high level of energy, which is virtually all dissipated as heat over a restricted area. The resulting temperatures can cause various types of surface damage such as burning with steels, softening (tempering) of the surface larger with possible rehardening, unfavorable residual tensile stresses, cracks, and distortions (Malkin, 1984).

2.4 GRINDING PARAMETERS

There are a few of parameters need to be considered in order to do grinding process such as the component centre height, h, longitudinal dressing feed-rate, f_d, the control wheel speed, n_r, the in-feed speed, v_{fa}, depth of cut and many more. When the process planner has a prior knowledge about the product quality likely to be produced on a component during grinding, optimum process sequence design and process parameter selection is feasible. A need therefore exists to develop intelligent predictive product quality performance and the process conditions. The qualities of machined parts play a crucial role in the functional capacity of the part and therefore, a great deal of attention should be paid to keep consistent tolerances (Malkin, 1984). The machining process has an important place in the traditional production industry. Cost effectiveness of all machining process has been eagerly investigated. This is mainly affected selection of suitable machining parameters like cutting speed, feed rate and depth of cut according to cutting tool and workpiece material. The selection of optimum machining parameters will result in longer tool life, better surface finish and higher removal rate (Cakir et al., 2007).

Depth of Cut: The increase in depth of cut during grinding process increases the surface roughness value and roundness error. Effect of depth of cut is an important aspect on roundness error (Malkin, 1984). This is because of more metal removal at higher depth of cut.

Grinding Feed Rate: When feed rate is increased, the arithmetic mean roughness value (R_a) also increased and gives poor finish. Because of higher feed rate the metal removal is not uniform and it may not remove the material and also due to high vibration of grinding machine which result in the bad quality product, i.e. - high surface roughness and roundness error (Malkin, 1984).

Material Removal Rate: High efficiency deep grinding with its high material removal rate offers the potential to improve cycle times whilst maintaining surface integrity, form and finish requirements (Comley et al., 2006).

Surface Roughness: Grinding is used in the metal working industry to produce parts of high quality surface finish and geometry. Surface roughness is one of the most important factors for evaluating workpiece quality during the finishing process because the quality of surface affects the functional characteristics of the workpiece such as fatigue and fracture resistance and surface friction (Samhouri and Surgenor, 2005). Surface roughness is one of the most important factors of workpiece in grinding process. The ground surface is affected by the wheel surface and wheel should be dressed before the ground surface deteriorates beyond a quality limit of surface integrity. The surface roughness of workpiece in grinding process is influenced and determined by the disc dressing conditions due to effects of dressing process on the wheel surface topography. In this way, prediction of the surface roughness helps to optimize the disc dressing conditions to improve surface roughness (Baseri et al., 2008).

2.5 SELECTION OF THE GRINDING WHEEL

A successful grinding is based on a qualified operator who has strong knowledge about the shapes, types and the properties of the grinding wheels and people have to know how to use all kinds of wheels in different conditions.

2.5.1 Grinding Wheel

The most typical materials for the grinding wheel are aluminium oxide and silicon carbide. The material of aluminium oxide is not as hard and fragile as silicon carbide, it is suitable for grinding the metals with high anti-tensile strength such as softer metal, forge iron and bronze. The crystals of the silicon carbide are very fragile. It is suitable for grinding the metals with high anti-tensile strength such as steel, marble and glass. The grinding wheel is a bonded abrasive body consisting usually of Al_2O_3 or SiC abrasive grain in a matrix of ceramic, resinoid, or rubber band. Wheels are available in different grit sizes and type and in different wheel grades and structures that is amounts of bond and porosity, both of which affect the performance and wear characteristics of the wheel (Middle, 2005).

2.5.2 Grain Density

The grain density is denominated by the sifting capacity, for example, a grain has the grain density 24 that means it passed a sifter with 24 net-eye/inch. The remaining rough grain density wheels are used for parts that need no fine finishing.

2.5.3 Aluminium Oxide Grinding Wheel

Aluminium oxide, the most common industrial mineral in use today, is used either individually or with other materials to form ceramic grains. As an angular, durable blasting abrasive, aluminium oxide can be recycled many times. It is the most widely used abrasive grain in sand blast finishing and surface preparation because of its cost, longevity and hardness. Harder than other commonly used blasting materials, aluminium oxide grit powder penetrates and cuts even the hardest metals and sintered carbide. Aluminium 50% lighter than metallic media, aluminium oxide abrasive grain has twice as many particles per pound. The fast-cutting action minimizes damage to thin materials by eliminating surfaces stresses caused by heavier, slower cutting media. Aluminium oxide grit powder has a wide variety of applications, from cleaning engine heads, valves, pistons and turbines blades in the aircraft industry to lettering in monument and marker inscriptions. It is also commonly used for matte finishing as well as cleaning and preparing parts for metalizing, plating and welding.

2.5.4 Silicon Carbide Grinding Wheel

Silicon carbide grinding wheels are tools used in manufacturing industry to form precision components and continue to be used to increased production rates due to their ability to remove high volumes of material at high speeds (Jackson, 2010). Silicon carbide is the hardest blasting media available. High-quality silicon carbide media is manufactured to a blocky grain shape that splinters. The resulting silicon carbides abrasive has sharp edges for blasting. Silicon carbide has a very fast cutting speed and can be recycled and reused many more times than sand. The hardness of silicon carbide allows for much shorter blast times relative to softer media. Silicon carbide grit is the ideal media for use on glass and stone in both suction or siphon and direct pressure blast

systems. The ability to be recycled multiple times results in a cost-effective silicon carbide grit blast media with optimal etching results. Since silicon carbide grit is harder than aluminium oxide, it can be used efficiently for glass engraving and stone etching. Silicon carbide grit blast media has no free silica, does not generate static electricity and is manufactured to contain minimal magnetic content.

2.6 SELECTION OF CUTTING FLUID

During machining operation, friction between workpiece-cutting tool and cutting tool-chip interfaces result high temperature on cutting tool. The effect of this generated heat affects shorter tool life, higher surface roughness and lowers the dimensional sensitiveness of work material. This result is more important when machining of difficult to cut materials, due to occurrences of higher heat (Cakir et al., 2007). The influence of cutting fluids on surface finish is relatively small and, in general fluids with greater lubricating action impart a somewhat better finish. The more important point is to ensure proper filtration of the fluid because suspended particles of abrasive and metal can cause deep scratches. Isolated scratch marks are a sure sign of dirty fluid. The remedy in such cases is to clean the tank and use magnetic separators at frequent intervals. The cutting fluids applied in machining processes basically have three characteristics which is cooling effect, lubricating effect and taking away formed chip from the cutting zone.

2.6.1 Cooling effect

It is necessary to decrease the effects of temperature on cutting tool and machined workpiece. Therefore, a longer tool life will be obtained due to less tool wear and the dimensional accuracy of machined workpiece will be improved.

2.6.2 Lubrication effect

This will cause easy chip flow on the rake face of cutting tool because of low friction coefficient. This would also result in the increased by the chips. Moreover, the influence of lubrication would cause less built-up edge when machining some materials

such as aluminium and its alloys. As a result, better surface roughness would be observed by using cutting fluids in machining processes.

2.6.3 Taking away formed chip from the cutting zone

It is also necessary to take the formed chip away quickly from cutting tool and machined workpiece surface. Hence the effect of the formed chip on the machined surface would be eliminated causing poor surface finish. Moreover part of the generated heat will be taken away by transferring formed chip.

2.7 NANOFLUIDS

Nanofluids are a new class of solid-liquid composite materials consisting of solid nanoparticles with at least one critical dimension smaller than -100nm. Much attention has been paid in the past decade to this new type of composite material because of its enhanced properties and behavior associated with heat transfer (Ding et al., 2007). The enhanced thermal behavior of nanofluids could provide a basis for an enormous innovation for heat transfer intensification, which is major importance to a number of industrial sectors including transportation, power generation, micro-manufacturing thermal therapy for cancer treatment, chemical and metallurgical sectors. Connective heat transfer can be enhanced passively by changing flow geometry, boundry conditions, or by enhancing thermal conductivity of the fluid (Wang and Mujumdar, 2008). Convective heat transfer refers to heat transfer between a fluid and surface due to the macroscopic motion of the fluid relative to the surface (Ding et al., 2007).

2.8 PREPARATION METHOD FOR NANOFLUIDS

Nanofluids contains two-phase systems which is solid phase and liquid phase. Nanofluids have an ability in order to possess enhanced thermophysical properties such as thermal conductivity, thermal diffusivity, viscosity and convective heat transfer coefficients compared to those of base fluids oil or water. It has proven its potential in

many fields. There are two methods in order to prepare the stability mechanisms in nanofluids.

2.8.1 Two steps method

The preparation of nanofluids begins by mixing of the base fluid with the nanomaterials. In the first step, nanomaterials are synthesized and obtained as powders, which are then introduced to the base fluid in the second step. This kind of method is the most widely used method in order for preparing nanofluids. Nanoparticles, nanofibers, nanotubes or other nanomaterials used in this method are first produced as dry powders by chemical or physical methods. The nanosized powder then dispersed into a fluid in the second processing step with the help of intensive magnetic force agitation, high shear mixing, homogenizing, and ball milling. This method is the most economic method to produce nanofluids in large scale, because nanopowder synthesis technique has been scaled up to industrial production level (Zu et al., 2009).

2.8.2 One step method

The one-step process consists of simultaneously making and dispersing the particles in the fluid. The process of drying, storage, transportation and dispersion of nanoparticles are avoided in this method in order to minimize the agglomeration of nanoparticles, and the stability of fluids can be increased. One-step physical method cannot synthesize nanofluids in large scale, and the cost is also high, so the one-step chemical method is developing rapidly (Zu et al., 2009). In contrast, the one-step method entails the synthesis of nanoparticles directly in the heat transfer fluid.

2.9 RESPONSE SURFACE METHOD

There are many statistical approaches of assessment of effect process parameters. Response surface methodology (RSM) is a collection of statistical technique useful for analyzing the effects of several independent variables on the response (Box and Draper, 1987). RSM has an important application in the process design and optimization as well as the improvement of existing design. This

methodology is more practical compared to theoretical models as it arises from experimental methodology which includes interactive effects of the variables and eventually, it depicts the overall effects of the parameters on the process.

2.10 ARTIFICIAL NEURAL NETWORK

The human brain provides proof of the existence of massive neural networks that can succeed at those cognitive, perceptual, and control tasks in which humans are successful. The brain is capable of computationally demanding perceptual acts and control activities. The advantage of the brain is its effective use of massive parallelism, the highly parallel computing structure, and the imprecise information-processing capability. The human brain is a collection of more than 10 billion interconnected neurons. Each neuron is a cell that uses biochemical reactions to receive process and transmit information. Artificial neural networks have been developed as generalizations of mathematical models of biological nervous systems (Abraham, 2005).

2.11 RADIAL BASIS FUNCTION

Radial basis functions emerged as a variant of artificial neural network in late 80's. However, their roots are entrenched in much older pattern recognition techniques as for example potential functions, clustering, functional approximation, spline interpolation and mixture models (Tou and Gonzalez, 1974). RBF's are embedded in a two layer neural network, where each hidden unit implements a radial activated function. The input into an RBF network is nonlinear while the output is linear (Park and Sandberg, 1991). The batch back propagation algorithm is used in layered feed-forward ANNs. This means that artificial neurons are organized in layers, and send their signals forward, and then errors are propagated backwards. The network receives inputs by neurons in the input layer, and the output of the network is given by the neurons on an output layer. There may be one or more intermediate hidden layers. The batch back propagation algorithm uses supervised learning, which means that we provide the algorithm with examples of the inputs and outputs we want the network to compute, and then the error (difference between actual and expected result) is calculated. The idea of the batch back propagation algorithm is to reduce this error, until the ANN learns the

training data. The training begins with random weights, and the goal is to adjust them so that the error will be minimal (Rumelhart and McClelland, 1986).

CHAPTER 3

METHODOLOGY

3.1 INTRODUCTION

This chapter discussed about the overall work flow progress of the project which is the preparation of workpiece, nanocoolant which is water-based SiO_2 nanocoolant, the flow of experiment done using the appropriate apparatus. Optimization of abrasive machining of ductile cast iron using water-based SiO_2 nanoparticles are used a Radial Basis Functions approach. There are several parameters for grinding process that had to be considering in this project in order to optimize the workpiece such as the depth of cut, table speed and type of coolant. This is important to ensure the quality of the product is in the best condition. However, the wheel speed needs to be constant due to the lack of machine used in the lab. The appropriate apparatus and experimental setup need to be prepare in order to achieve the objectives of this research paper. Thus, the collected data will be analyzed further and interpreted in suitable way to validate the data by compare with previous research.

3.2 WORKPIECE PREPARATION

A block of the ductile cast iron is taken from the foundry lab. In order to prepare the workpiece, the workpiece was cut by the disc cutter into two parts so that it is easy to further for the next stage seems the block of the workpiece are big in size. Figure 3.1 shows the disc cutter machine. The small pieces of the separated workpiece then undergo grinding process in order to get the flat surface. The compositions are afterwards made to the workpiece to test the quality of the workpiece. Composition is defined as something formed in the manner or the resulting state or quality. We had

been taking six shots of composition in order to test the quality of the workpiece. Workpiece is then undergoing squaring process using the milling machine. Figure 3.2 shows the operation of Squaring using the milling machine. Milling is a machining operation in which a workpiece is fed past a rotating cylindrical tool with multiple cutting edges. The axis of rotation of the tool is perpendicular to the feed direction. In this experiment, milling process are using in order to get the squaring surface and to remove the ingots and to get the 60 mm × 30 mm × 20 mm dimension of the workpiece. Figure 3,3 shows the milling machine. The workpiece is then undergoing the band saw machine operation. Band saw machine is a machine tool designed to cut material to a desired length or contour. This kind of machine is faster and easier than hand sawing and is used principally to produce an accurate square or mitered cut on the workpiece. The band saws are two common types of sawing machines used to cut metal in the machine shop. The band saw uses a reciprocating which is back and forth cutting action similar to the one used in a hand hacksaw. It is used for square or angle cutting stock. Figure 3.4 shows the operations of the band saw cutting the workpiece.

Figure 3.1: Disc Cutter

Metal-cutting band saw machines fall into two basics categories which is vertical machines and horizontal machines. For this experiment, band saw machine are used to cut the material into small pieces. Figure 3.5 shows band saw machine (EVERISING S-300HB). The horizontal band saw machine was used in this experiment. It is actually a continuous band which revolves around a drive wheel and

idler wheel in the band support frame. Two band guides use rollers to twist the band so that the teeth are in the proper cutting position. The guides are adjustable and should adjust so that they are slightly further apart than the width of the material to be cut. This will give maximum support to the saw band and help assure a straight cut.

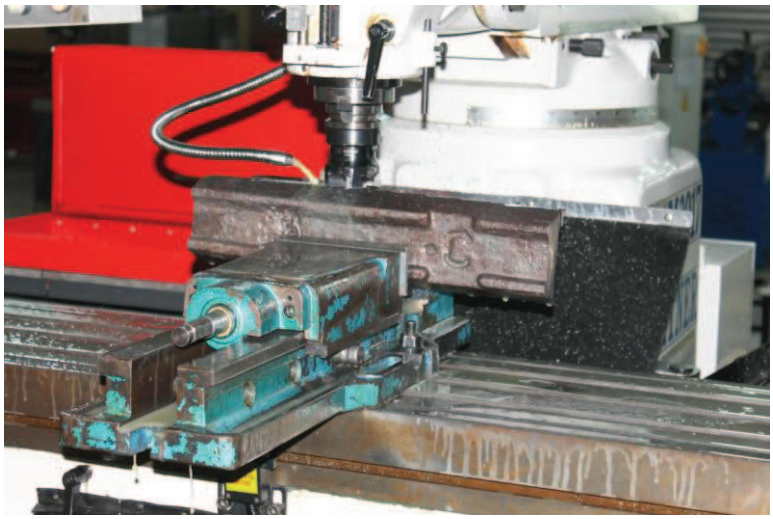

Figure 3.2: Squaring using the milling machine

Figure 3.3: Milling Machine (PARTHNER)

Figure 3.4: Operations of the band saw cutting the workpiece

Figure 3.5: Band saw machine (EVERISING S-300HB)

3.3 EXPERIMENTAL DETAILS

For this experiment, the Precision Surface Grinding Machine (STP-1022ADCII) was used. Surface grinding machines and processes are where first developed to manufacture very tight tolerances, smooth surface finishes, and removing material from very hard materials.

(a)

(b)

(c)

Figure 3.6: Precision Surface Grinding Machine (STP-1022ADCII)

The grinding table is then measured using the Tachometer to measure its speed. Figure 3.7 shows the tachometer which is an instrument to measures the rotation speed of a shaft or disk. In other words, tachometers are utilized to measure the rotating speed of any device. By using the tachometer, the speed of the machine is measured in RPM. For the experiment, the temperatures of the workpiece need to be taken using infra-red thermometer. This is important to record the data in the table for the analysis. Figure 3.8 shows the infra-red thermometer.

Figure 3.7: Tachometer

Figure 3.8: Infra-red thermometer

Grinding wheels are made from many types of grit in a wide range of sizes, in conjunction with many bond materials and compositions. For this experiment, the silicon carbide abrasive wheels are used for both conventional and nanocoolant grinding. Figure 3.9 shows Silicon carbide grinding wheel. Conventional abrasive wheels usually comprise the entire bonded abrasive structure. The different type of grinding wheels together with the requirement of a wide variety of wheel shapes and sizes to fit all the diverse grinding machines and jobs to be done.

Conventional Abrasives Wheel Specification: It is convenient to refer to the standard marking system for specifying conventional grinding wheels. The wheel specification defines the following parameters:

i) the type of abrasive in the wheel
ii) the abrasive grain size
iii) the wheel's hardness
iv) the wheel's structure
v) the bond type

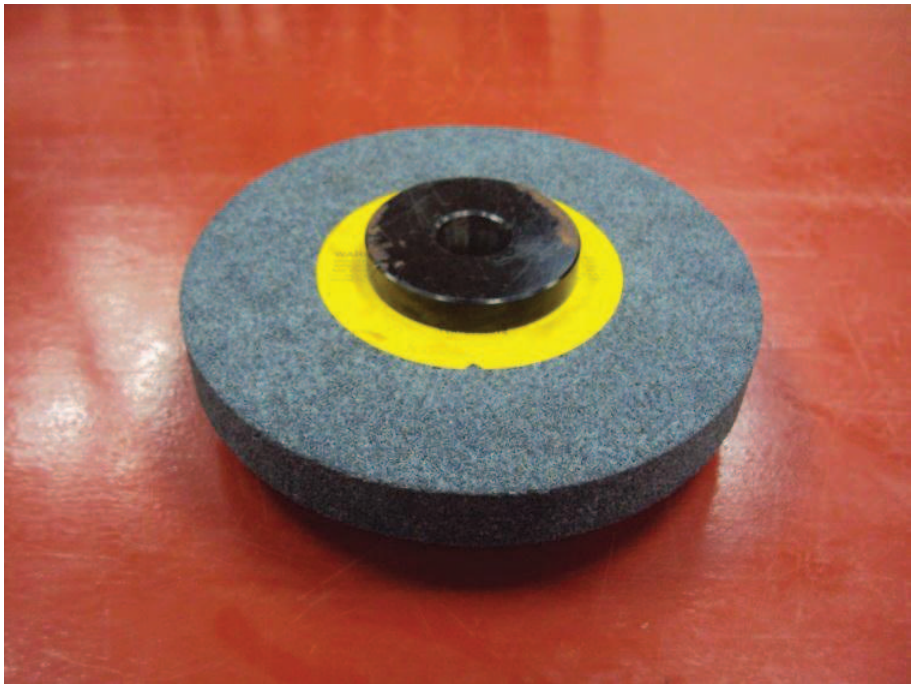

Figure 3.9: Silicon carbide grinding wheel

3.4 WATER BASED SiO_2 NANOCOOLANT PREPARATION

For the conventional grinding, the water based coolant used as the coolant. This is important so that the surface roughness of this conventional grinding can be compare with the surface roughness of nanocoolant grinding. Coolant or cutting fluid widely used in metal machining operations. The purpose of coolant are to wash away chips from the tool, reduce heat generated reduces, reduces frictions between tool and workpiece and also to enhanced tools life. Most of the machines are already installed with a coolant system by the manufactured factory itself. This water based coolant are contain of 60% of water and 40% of ethylene glycol. The coolant features usually has mild alkaline pH. It does not contain toxic elements like sulphur and chlorine. Coolant also devoid of bacterial growth due to its special additives. It has an excellent anticorrosive property over a wide dilution range. As it is an aqueous base, it provides good cooling effect, which leads increase in the tool life. This coolant will also apply to the drilling, grinding, tapping, turning, milling and boring process. Figure 3.10 shows water based SiO_2 Nanocoolant.

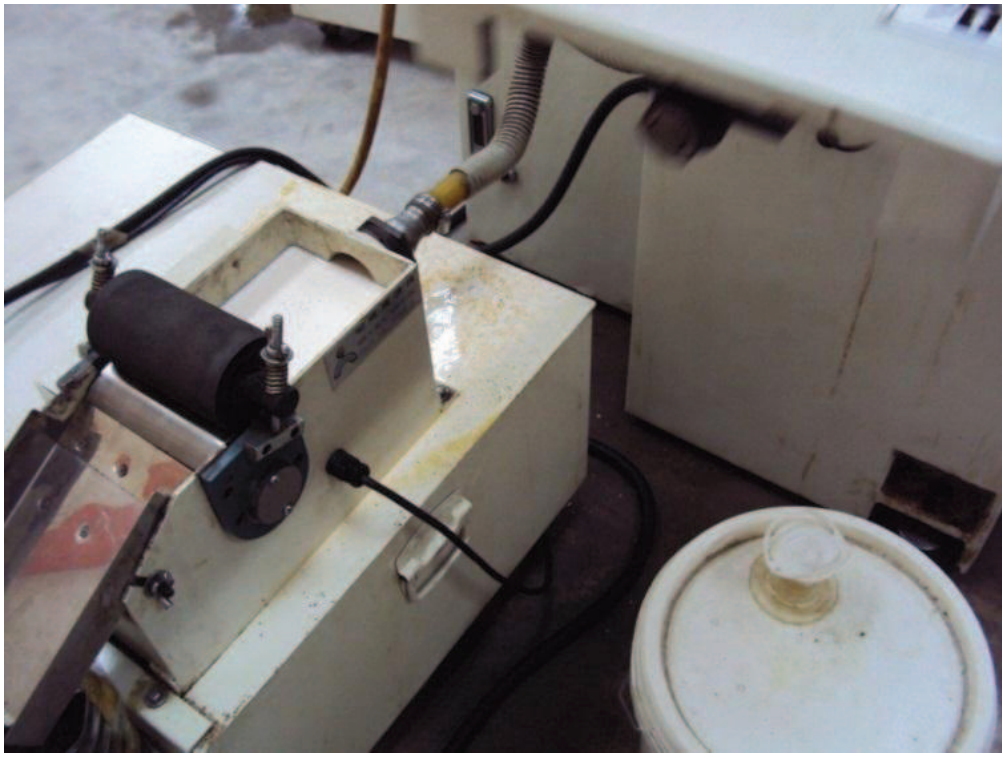

Figure 3.10: Water Based-Coolant

There are two methods in order to prepare the stability mechanisms of nanocoolant. They are two-step method and one-step method. For the two-step method, nanoparticles are comes directly as a dry powder from the supplier. Then, it is diluted the nanoparticles with the distilled water. The nanosized powder then dispersed in the distilled water in the second processing step with the help of intensive magnetic force agitation, high shear mixing, homogenizing, and ball milling. However, this method is economical in order to produce large scale of nanofluids. For this experiment, it is prepared the nanofluids using the one-step method since need a small scale of nanofluids. This process consists of simultaneously making and dispersing the particles in the fluid. Table 3.1 shows the properties of the SiO_2 nanoparticles. Figure 3.11 shows the prepeation of SIO2 nanofluids using one-step method.

Table 3.1: Properties of the SiO_2 nanoparticles

Weight Percent	25 wt%
Particle Size	30 nm
Density	2170-2660g/cm^3
pH	8-11 amorphous

Figure 3.11: SiO_2 nanocoolant preparation

3.5 SURFACE ROUGHNESS TESTER

Perthometer is a surface roughness measuring device. The Perthometer operates by drawing a stylus at constant speed across a 0.56 mm, 1.75 mm, 5.6 mm and 17.5 mm length of the surface. The diamond point has a diameter of 5 μm. The length of travel of the stylus is divided into 7 equal segments. The first and the last segments axis of the panel. A fifth trace was made in the center of the panel with the stylus movement perpendicular to the other traces. Measurements made on the backs were essentially the same as those made on the fronts. Profile parameter measurements were very consistent from one panel to the next. The blast cleaning process was very tightly controlled for each of the three blasting conditions, as the sequenced by the uniformly of the data. The data was tabulate in the table and will then analyze in the ANOVA. Figure 3.12 shows the surface roughness tester using Perthometer.

(a) Mahr Perthometer (b) Surface Perthometer

Figure 3.12: Surface roughness tester

3.6 SCANNING ELECTRON MICROSCOPE

Microstructure analysis is a procedure for testing and analyzing a prepared surface of a material. It can generate fine structural images of samples using optical microscopy, and combined with careful preparation of the samples, particularly cross-

sections, allows many aspects of the physical properties of a sample to be analyzed and explain. These include:

- Identification and elimination of defects such as contaminants, stains, cracks and flaws which can have catastrophic effects on products performances through stress concentrators.
- Failure investigations or evaluation of process improvements in products and processes.
- Microstructure analysis also includes measurement of more fundamentals material properties such as mechanical properties and hardness testing.

For this experiment, the microstructure analysis of three depth of cut (DOC) parameters thorough the workpiece had been performed which is 0.02 µm, 0.04 µm and 0.06 µm. Each of the depth of cut was magnified using the 200x and 700x magnifier of the microscope. Figure 3.13 shows the scanning electron machine.

Figure 3.13: Scanning electron machine

3.7 DESIGN OF EXPERIMENT

Before running the experiment, the design of experiment should be design first. This is important in order to simplify the experimental and analysis data. For this experiment, the JMP 9 software is used to generate the table of DOE. Table 2 shows the design of experiment.

Table 3.2: Design of Experiment

Table Speed (mm/s)	Depth of Cut (µm)
333.33	0.2
333.33	0.4
333.33	0.6
500	0.2
500	0.4
500	0.6
666.67	0.2
666.67	0.4
666.67	0.6

3.8 RESPONSE SURFACE METHODOLOGY

In multivariable systems, the classical approach of changing one variable at a time to study the effects on other variables for a particular response is time consuming. Therefore, an alternative strategy involving statistical approaches, e.g., response surface methodology (RSM) was applied to solve for multiple variables in this complex system. In this study, the central composite design (CCD) and response surface method were applied to optimize the most important operating variables which are table speed and depth of cut. Table 3.3 shows experimental values and coded levels of the independent variables. The behaviors of the system are described by using the first-order and second-order analysis. The first order equation is defined as Eq. (3.1).

$$y = \beta_0 + \beta_1 x_1 + \beta_2 x_2 + \varepsilon \qquad (3.1)$$

where y is the predicted response, β_0 is the interception coefficient, β_1 are the linear terms, β_2 are the quadratic terms, and ε indicates the interactions and the coded levels of the independent variables.

The second order equation is expressed as Eq. (3.2):

$$y = \beta_0 + \beta_1 x_1 + \beta_2 x_2 + \beta_{11} x^2_{11} + \beta_{22} x^2_{22} + \beta_{12} x_1 x_2 \quad + \varepsilon \qquad (3.2)$$

Table 3.3: Experimental values and coded levels of the independent variables

Variable symbol and unit	Independent Variable	Levels		
		-1	0	+1
Table Speed (mm/s)	X_1	333.33	500.00	666.67
Depth of Cut (μm)	X_2	0.02	0.04	0.06

3.9 ARTIFICIAL NEURAL NETWORK

An Artificial Neural Network (ANN), the most basic and commonly used is the multi-layer perception (MLP). It is consists of at least three or more layers which is input, output, and number of hidden layers. The batch back propagation is one of the famous training algorithms for MLP. For this project, the gradient is determined using a technique called batch back propagation, which involves performing computations backward through the network. Once the network weights and biases are initialized, the network is ready for training. The network can be trained for function approximation which is nonlinear regression, pattern association, or pattern classification. The training process requires a set of examples of proper network behavior network inputs and target outputs. During training the weights and biases of the network are iteratively adjusted to minimize the network performance function. The performance function for feed forward network is mean square error which means the average squared error between the network outputs and the target outputs. All these algorithms use the gradient of the performance function to determine how to adjust the weights to minimize performance. The objective of developed ANN is to predict the surface roughness and MRR for conventional and nanocoolant grinding. The available data set from the experimental

study was divided into two sets; training and testing sets. The experimental data set consists of 9 values each due to its grinding passes and types of coolant. The ANN model was trained using 5 randomly selected data (accounting for 50% of the total data) while the remaining four data (accounting for 25% each) was utilized for testing and validation of the network performance.

There are many variations of the batch back propagation algorithm. The simplest implementation of batch back propagation learning updates the network weights and biases in the direction function decreases most rapidly, the negative of the gradient. There are two different ways in which this gradient descent algorithm can be implemented: incremental mode and batch mode. In incremental mode, the gradient is computed and the weights are updated after each input is applied to the network before the weights are updated. In batch mode, the weights and biases of the network are updated only after the entire training set has been applied to the network. The gradients calculated at each training example are added together to determine the change in the weights and biases. The primary objective in the batch back propagation is to explain how to use the batch back propagation training functions in the toolbox to train the feed forward neural networks to solve specifics problems. There are generally four steps in the training process which are:

a) Assemble the training data

The network uses the batch back propagation algorithm for training. The application randomly divides input vectors and target input vectors from the experimental data.

-50% from the data are used for training.
-25% from the data are used to validate that the network is generalizing and to stop training before overfitting.
-The rest 25% are used as a completely independent test of network generalization.

b) Create the network

The architecture of the developed ANN model is shown in Figure 3. 14.

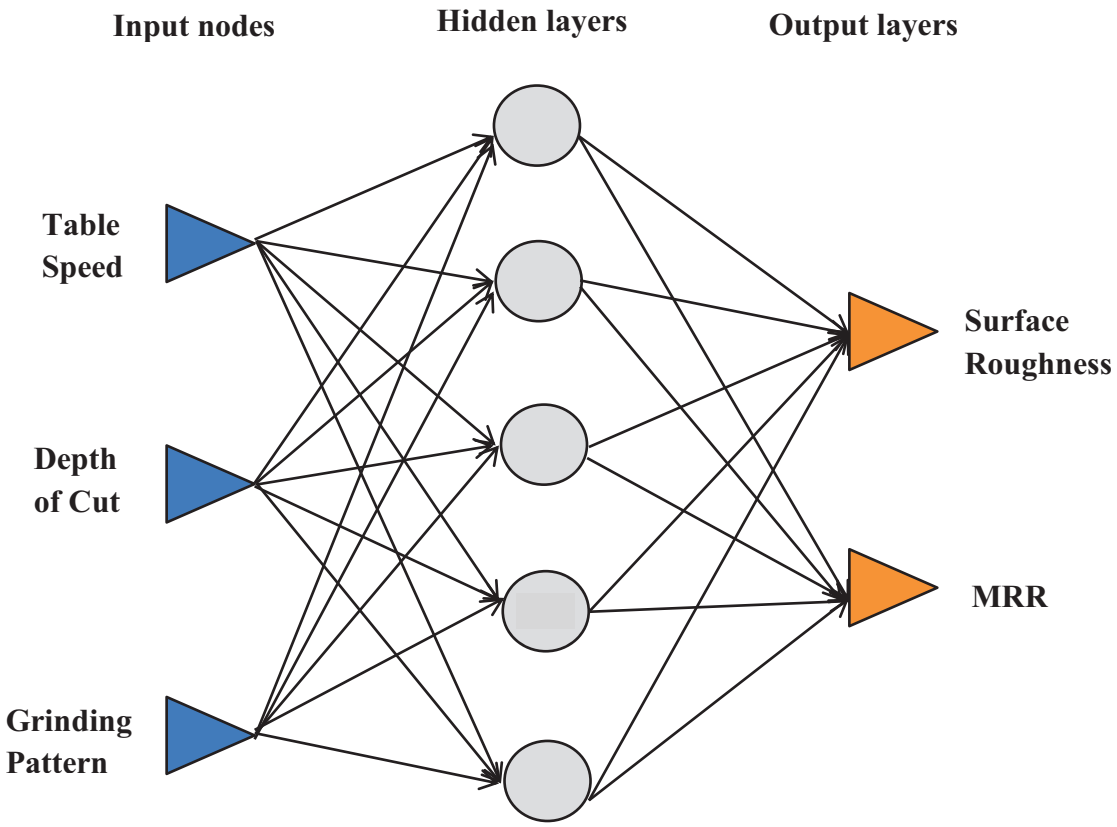

Figure 3.14: The architecture of developed ANN model

c) Train the network

During training, the training progress and allows interrupting training at any point by clicking stop training. For this experiment we are using the batch back propagation algorithm. This training stopped when the validation error increase which occurred at iteration 5000. The BP learning algorithms has been used in feed-forward. Optimal number of the neurons in the hidden layer was determined by trying different networks. The number of neurons is increased from 3 to 7 based on the trial and error method in the hidden layer for each analysis (Huseyin and Kayfeci, 2009).

3.10 DATA ANALYSIS

Data in Table 3.4-3.7 show the experimental results of the surface roughness and material removal rate for conventional and nanofluid coolant. The 0.02 µm, 0.04 µm and 0.06 µm for the depth of cut and 333.33 mm/s, 500 mm/s, and 666.67 mm/s for the table speed were set.

Table 3.4: Experimental results for conventional-Single pass

Work piece	Table speed (mm/s)	Depth of Cut (µm)	Time Taken (s)	Mass Different (g)	Density of Cast Iron (g/cm^3)	MRR (cm^3/s)	Surafce Roughness (µm)
A	333.33	0.02	0.85	0.152	7.2	0.025	0.304
B	333.33	0.04	0.85	0.308	7.2	0.050	0.321
C	333.33	0.06	0.85	0.453	7.2	0.074	0.489
D	500.00	0.02	0.64	0.147	7.2	0.032	0.241
E	500.00	0.04	0.64	0.302	7.2	0.066	0.265
F	500.00	0.06	0.64	0.447	7.2	0.097	0.286
G	666.67	0.02	0.42	0.138	7.2	0.046	0.151
H	666.67	0.04	0.42	0.293	7.2	0.097	0.181
I	666.67	0.06	0.42	0.475	7.2	0.158	0.237

Table 3.5: Experimental results for Silicon Oxide nanocoolant-Single pass

Work piece	Table speed (mm/s)	Depth of Cut (µm)	Time Taken (s)	Mass Different (g)	Density of Cast Iron (g/cm^3)	MRR (cm^3/s)	Surafce Roughness (µm)
A	333.33	0.02	0.80	0.062	7.2	0.011	0.39
B	333.33	0.04	0.80	0.146	7.2	0.025	0.405
C	333.33	0.06	0.80	0.281	7.2	0.049	0.468
D	500.00	0.02	0.62	0.062	7.2	0.014	0.292
E	500.00	0.04	0.62	0.023	7.2	0.005	0.381
F	500.00	0.06	0.62	0.27	7.2	0.060	0.388
G	666.67	0.02	0.44	0.049	7.2	0.015	0.189
H	666.67	0.04	0.44	0.011	7.2	0.003	0.245
I	666.67	0.06	0.44	0.178	7.2	0.056	0.277

Table 3.6: Experimental results for conventional-Multiple pass

Work piece	Table speed (mm/s)	Depth of Cut (µm)	Time Taken (s)	Mass Different (g)	Density of Cast Iron (g/cm^3)	MRR (cm^3/s)	Surafce Roughness (µm)
A	333.33	0.02	0.87	0.204	7.2	0.033	0.316
B	333.33	0.04	0.87	0.354	7.2	0.057	0.336
C	333.33	0.06	0.87	0.512	7.2	0.082	0.402
D	500.00	0.02	0.65	0.196	7.2	0.042	0.224
E	500.00	0.04	0.65	0.347	7.2	0.074	0.226
F	500.00	0.06	0.65	0.498	7.2	0.106	0.276
G	666.67	0.02	0.42	0.192	7.2	0.063	0.186
H	666.67	0.04	0.42	0.342	7.2	0.113	0.189
I	666.67	0.06	0.42	0.487	7.2	0.161	0.233

Table 3.7: Experimental results for Silicon Oxide nanocoolant- Multiple pass

Work piece	Table speed (mm/s)	Depth of Cut (µm)	Time Taken (s)	Mass Different (g)	Density of Cast Iron (g/cm^3)	MRR (cm^3/s)	Surafce Roughness (µm)
A	333.33	0.02	0.84	0.071	7.2	0.012	0.351
B	333.33	0.04	0.84	0.228	7.2	0.038	0.372
C	333.33	0.06	0.84	0.473	7.2	0.078	0.374
D	500.00	0.02	0.68	0.21	7.2	0.043	0.314
E	500.00	0.04	0.68	0.245	7.2	0.050	0.336
F	500.00	0.06	0.68	0.114	7.2	0.023	0.361
G	666.67	0.02	0.47	0.361	7.2	0.107	0.238
H	666.67	0.04	0.47	0.304	7.2	0.090	0.283
I	666.67	0.06	0.47	0.208	7.2	0.061	0.293

CHAPTER 4

RESULTS AND DISCUSSION

4.1 INTRODUCTION

This chapter is to analyze the results of the experiment and their discussion. The method used is response surface methodology and artificial neural network using radial basis function network. RSM has an important application in the process design and optimization as well as the improvement of existing design. This methodology is more practical compared to theoretical models as it arises from experimental methodology which includes interactive effects of the variables and eventually, it depicts the overall effects of the parameters on the process (Fristak et al., 2012). Artificial neural network (ANN) model has been developed. The radial basis function (RBF) network is a three-layer feed-forward that uses a linear transfer function for the output units and a nonlinear transfer function (normally the Gaussian) for the hidden layer neurons. Radial basis network may require more neurons than standard feed-forward back propagation networks, but often they can be designed with lesser time. They perform well when many training data are available (Abraham, 2005).

In order to achieve the objective of the uncertainty analysis and to get a good result, there are a few step that required which are selecting the parameters and defined the input and output data. For the second step are applied the analytical and numerical theory with manual calculation in the Excel. The predicted results are compared with the experimental value by calculating percentage of error.

4.2 MATHEMATICAL MODELING

After conducting the conventional coolant and SiO_2 nanocoolant grinding with single and multiple grinding patterns, the experimental data were used to find parameters appearing in postulated first order model (FOM) and second order model (SOM). RSM comprises a body of methods for exploring for optimum operating conditions through experimental methods.

4.2.1 First-Order Modeling

Table 4.1 and Table 4.2 are presented the ANOVA results for conventional coolant and SiO_2 nanocoolant respectively. The R^2 is 0.98 and the RMSE is just 0.0075. The P-value for MRR recorded 0.001 and the P-value of lack of fit recorded 0.7557 (Table 4.1). The R^2 is 0.65 and the RMSE is just 0.0155. The P-value of lack of fit recorded 0.7623 (Table 4.2). Regression equation with low P-value (<0.05) indicates that the model is considered to be statistically significant (Fristak et al., 2012). Value of $P < 0.0001$ indicates statistical significance of a quadratic model. On the basis of this investigation, the relationship between the independent variables (table speed, depth of cut) and the response (surface roughness, MRR) can be explained according to the regression model. The goodness of the model can be confirmed by the coefficient of determination R^2 are close to 1, which are very high indicate a high correlation between the experimental and predicted values. However, there are two outleirs at the graph which indicates the insignificant of the results due to the error during the experiment. Figure 4.1(c) shows the result of multiple pass of conventional grinding. The R^2 is 0.97 and the RMSE is just 0.0074. The p-value of ANOVA recorded 0.001 and the p-value of lack of fit recorded 0.8726 (Table 4.1). Figure 4.1(d) shows the result of multiple pass of silicon oxide nanocoolant grinding. The R^2 is 0.73 and the RMSE is 0.0191. The p-value of ANOVA recorded 0.0379 and the p-value of lack of fit recorded 0.3655 (Table 4.2). Just like Figure 4.1(b), there are also two outliers at the graph which indicates the insignificant of the results due to the error during the experiment.

Table 4.1: ANOVA results for conventional coolant grinding

Source	Degree of freedom	Sum of sq.	F-static	P-value
Single pass grinding				
Model	3	0.01323234	78.0739	<.0001
Error	6	0.00033897		
C Total	9	0.01357131		
Lack-of-Fit	5	0.00025144	0.5745	0.7557
Pure Error	1	0.00008753		
Total Error	6	0.00033897		
Multiple pass grinding				
Model	3	0.01266105	77.8424	<.0001
Error	6	0.00032530		
C Total	9	0.01298635		
Lack-of-Fit	5	0.00019517	0.3000	0.8726
Pure Error	1	0.00013013		
Total Error	6	0.00032530		

Table 4.2: ANOVA results for SiO_2 nanocoolant grinding

Source	Degree of freedom	Sum of sq.	F-static	P-value
Single pass grinding				
Model	3	0.00263589	3.6429	0.0834
Error	6	0.00144714		
C Total	9	0.00408303		
Lack-of-Fit	5	0.00106445	0.5563	0.7623
Pure Error	1	0.00038269		
Total Error	6	0.00144714		
Multiple pass grinding				
Model	3	0.00594974	5.4442	0.0379
Error	6	0.00218572		
C Total	9	0.00813546		
Lack-of-Fit	5	0.00209623	4.6849	0.3365
Pure Error	1	0.00008949		
Total Error	6	0.00218572		

The mathematical model of material removal rate for conventional coolant and SiO_2 nanocoolant with single pass and multiple pass grinding as follows:

$$\mathrm{MRR}_{\mathrm{Conv-}-single\mathrm{pass}} = 0.07220 + 0.02507 \times Table\ Speed + 0.03762 \times Depth\ of\ Cut + Table\ Speed \times (Depth\ of\ Cut \times 0.01556) \quad (4.1)$$

$$\mathrm{MRR}_{\mathrm{Conv-multiplepass}} = 0.08212 + 0.02780 \times \mathit{Table\ Speed} + 0.03521 \times \mathit{Depth\ of\ Cut} + \mathit{Table\ Speed} \times (\mathit{Depth\ of\ Cut} \times 0.01210) \quad (4.2)$$

$$\mathrm{MRR}_{\mathrm{SiO2-singlepass}} = 0.02737 + -0.00163 \times \mathit{Table\ Speed} + 0.02089 \times \mathit{Depth\ of\ Cut} + \mathit{Table\ Speed} \times (\mathit{Depth\ of\ Cut} \times 0.00067) \quad (4.3)$$

$$\mathrm{MRR}_{\mathrm{SiO2-multiplepass}} = 0.05383 + 0.02172 \times \mathit{Table\ Speed} + 0.000275 \times \mathit{Depth\ of\ Cut} + \mathit{Table\ Speed} \times (\mathit{Depth\ of\ Cut} \times -0.02792) \quad (4.4)$$

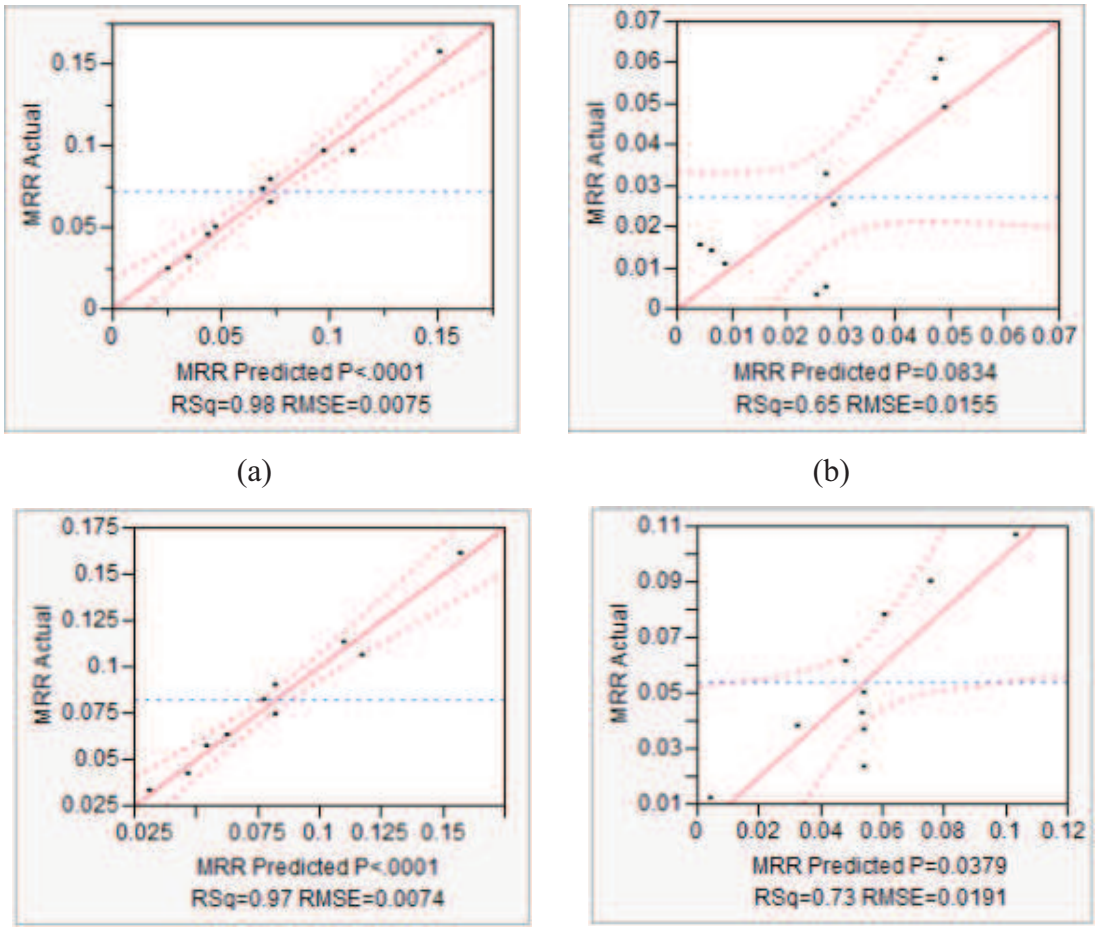

Figure 4.1: (a): Conventional-Single pass, (b): SiO_2-Single pass, (c): Conventional-Multiple pass, (d): SiO_2-Multiple pass

Figure 4.2 shows the trends of surface plot of the depth of cut and table speed versus material removal rate. The depth of cut is inversely proportional with the material removal rate. As the DOC is increase, the specimen surface is smoother.

Different with the table speed, it is directly proportional with the MRR. The increasing in the table speed, will give the high value of MRR.

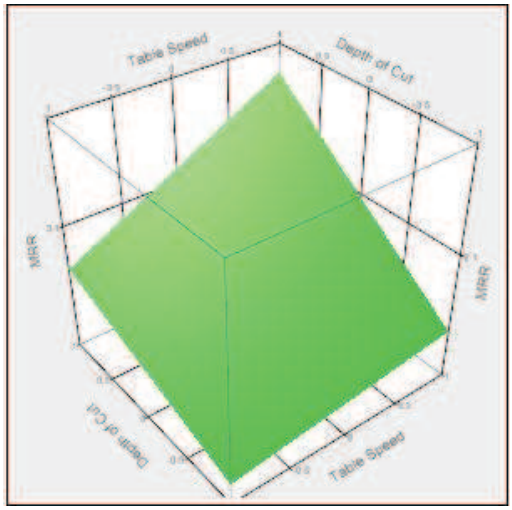

(a) Conventional-Single pass

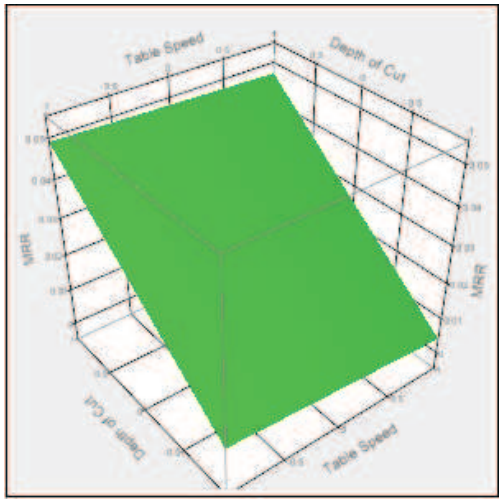

(b) SiO_2-Single pass

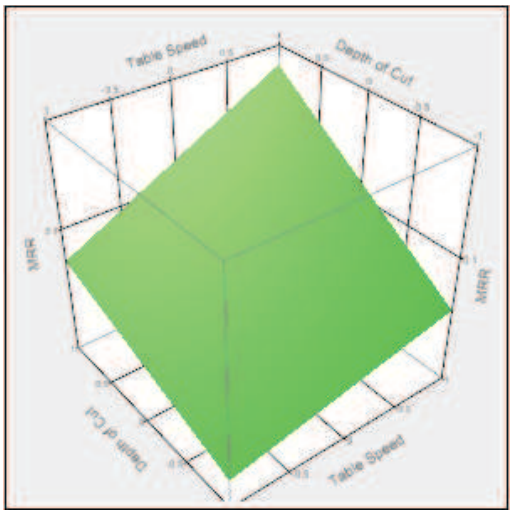

(c) Conventional-Multiple pass

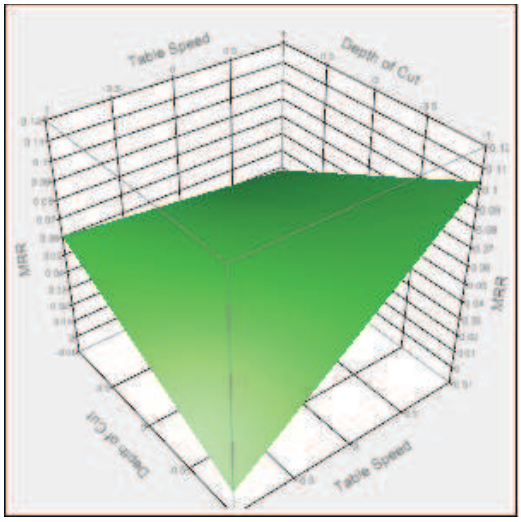

(d) SiO_2-Multiple pass

Figure 4.2: Contour plot for first order RSM model

4.2.2 Second Order Modeling

Table 4.3 and Table 4.4 are presented the ANOVA results for second order modeling of MRR for conventional coolant and SiO2 nanocoolant grinding respectively. The P-value of lack for both cases are more that 0.005. Therefore, both models are adequate and fit for analysis. Figure 4.3(b) shows the result of single pass silicon oxide nanocoolant grinding. Figure 4.3(c) shows the result of multiple pass of

conventional grinding. However, there are one outleirs at the graph which indicates the insignificant of the results due to the error during the experiment. Figure 4.3(a), there are also one outleirs at the graph which indicates the insignificant of the results due to the error during the experiment. Figure 4.3(d) shows the result of multiple pass of silicon oxide nanocoolant grinding. Predicted values by SOM are found in good agreement with experimental readings (Table 4.3 and 4.4).

Table 4.3: ANOVA Results of second-order model for conventional grinding

Source	Degree of freedom	Sum of sq.	F-static	P-value
Single pass grinding				
Model	5	0.01334571	47.3250	0.0012
Error	4	0.00022560		
C Total	9	0.01357131		
Lack-of-Fit	3	0.00013807	0.5258	0.7383
Pure Error	1	0.00008753		
Total Error	4	0.00022560		
Multiple pass grinding				
Model	5	0.01279319	52.9849	0.0010
Error	4	0.00019316		
C Total	9	0.01298635		
Lack-of-Fit	3	0.00006303	0.1615	0.9114
Pure Error	1	0.00013013		
Total Error	4	0.00019316		

Table 4.4: ANOVA Results of second-order model for SiO_2 nanocoolant

Source	Degree of freedom	Sum of sq.	F-static	P-value
Single pass grinding				
Model	5	0.00342293	4.1484	0.0964
Error	4	0.00066010		
C Total	9	0.00408303		
Lack-of-Fit	3	0.00027741	0.2416	0.8625
Pure Error	1	0.00038269		
Total Error	4	0.00066010		
Multiple pass grinding				
Model	5	0.00761519	11.7096	0.0168
Error	4	0.00052027		
C Total	9	0.00813546		
Lack-of-Fit	3	0.00043078	1.6046	0.5125
Pure Error	1	0.00008949		
Total Error	4	0.00052027		

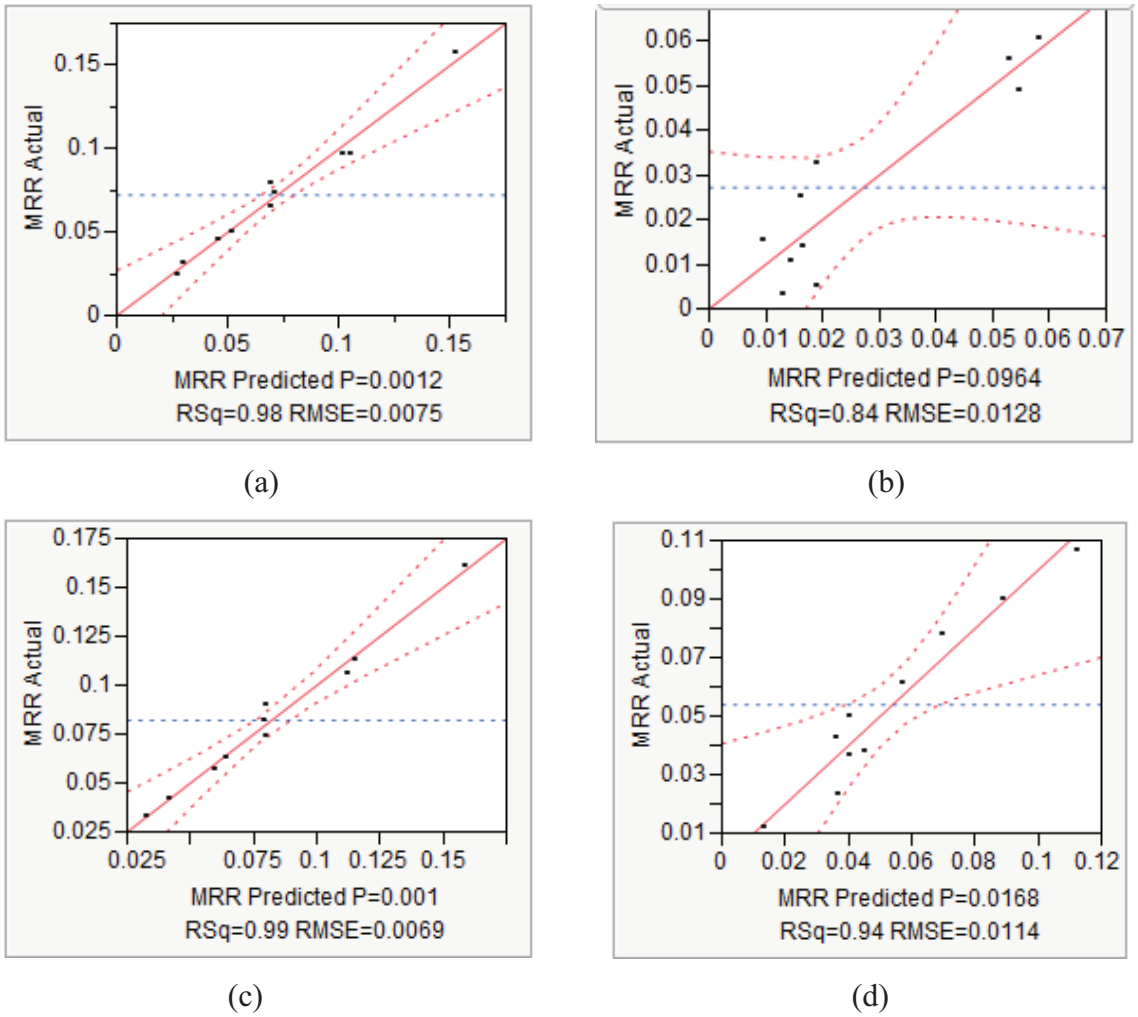

Figure 4.3: (a): Conventional-Single pass, (b): SiO_2-Single pass, (c): Conventional-Multiple pass, (d): SiO_2-Multiple pass

Figure 4.4 shows the trends of surface plot of the depth of cut and table speed versus material removal rate. The depth of cut is inversely proportional with the material removal rate. As the DOC is increase, the specimen surface will be smoother. Different with the table speed, it is directly proportional with the MRR. The increasing in the table speed, will give the high value of MRR. The mathematical model of material removal rate for conventional coolant and SiO_2 nanocoolant with single pass and multiple pass grinding as follows:

$$\begin{aligned} \mathrm{MRR}_{\mathrm{Conv-}single\mathrm{pass}} &= 0.06944 + 0.02507 \times TS + 0.03762 \times DOC \\ &+ TS \times (DOC * 0.01556) + TS \times (TS \times 0.00687) + DOC \times (DOC \times -0.00228) \end{aligned} \quad (4.5)$$

$$MRR_{Conv-multiplepass} = 0.01893 + -0.00163 \times TS + 0.02089 \times DOC + TS \times (DOC \times 0.00067) + TS \times (TS \times -0.00447) + DOC \times (DOC \times 0.01831) \quad (4.6)$$

$$MRR_{SiO2-singlepass} = 0.07993 + 0.02780 \times TS + 0.03521 \times DOC + TS \times (DOC \times 0.01210) + TS \times (TS \times 0.007148) + DOC \times (DOC \times -0.00351) \quad (4.7)$$

$$MRR_{SiO2-multiplepass} = 0.40203 + 0.02172 \times TS + 0.00027 \times DOC + TS \times (DOC \times -0.02792) + TS \times (TS \times 0.02671) + DOC \times (DOC \times -0.00397) \quad (4.8)$$

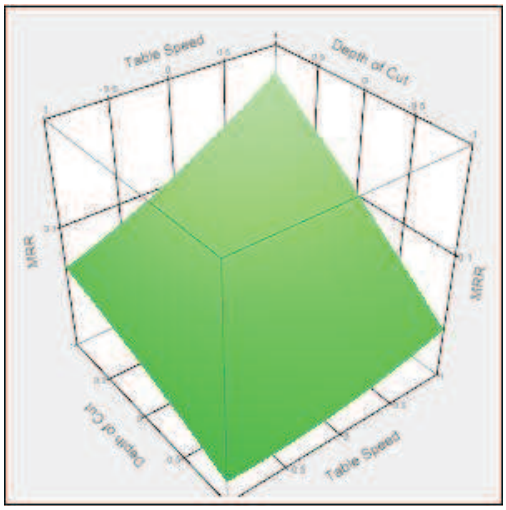

(a) Conventional-Single pass

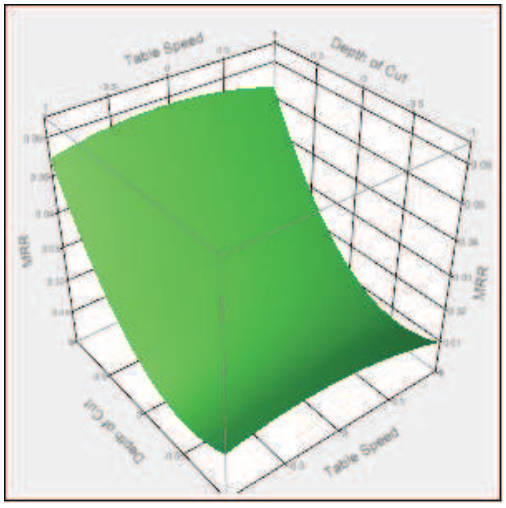

(b) SiO_2-Single pass

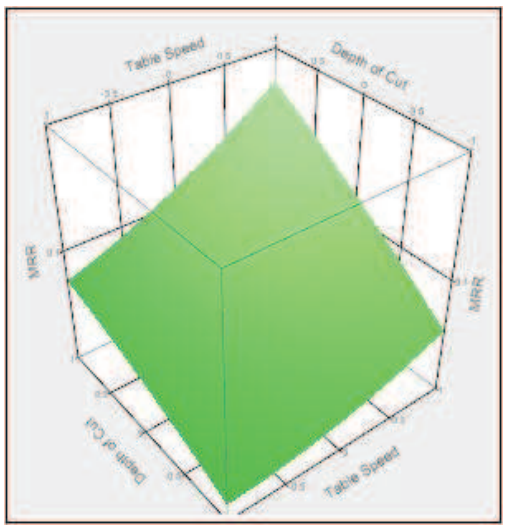

(c) Conventional-Multiple pass

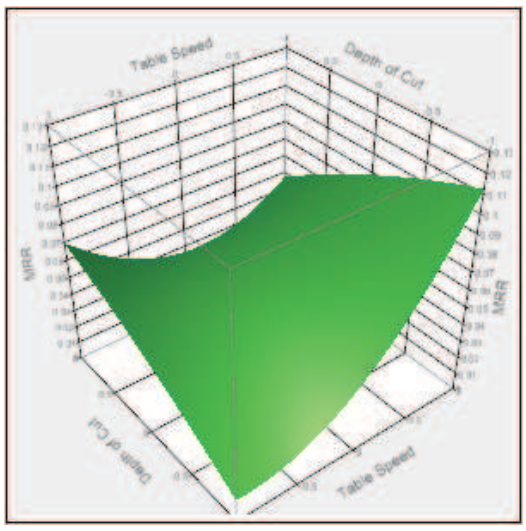

(d) SiO_2-Multiple pass

Figure 4.4: Contour plot for second order RSM model

4.3 ARTIFICIAL NEURAL NETWORK ANALYSIS

The ANN model is developed for predicting the surface roughness and MRR. The prediction of trained ANN for DOC and table speed is selected. To develop of ANN model, the network is processed through two stages which are training stage and testing/validation stage. In the training stage, the network is tested to stop or continue training it, and it is used to predict an output. It is also used to calculate different measures of error. The network training process is stopped when the testing error is within the tolerance limits. Table 4.5 and Table 4.6 present the architecture search of surface roughness and MRR for single pass conventional as well as SiO2 nancoolant respectively. ID 2 is selected for surface roughness and MRR prediction due to the highest R^2 values.

Table 4.5: Architecture search for conventional-Single Pass

ID	N	F	TE	VE	TE	C	R-S	SR
Surface Roughness								
1	1	0.993363	0.004693	0.050774	0.093447	0.999091	0.993363	AID
2	**18**	**0.998635**	**0.002059**	**0.031362**	**0.111193**	**0.999850**	**0.998635**	**AID**
3	11	0.804160	0.039303	0.032449	0.025787	0.945085	0.804160	AID
4	7	0.997642	0.002858	0.038934	0.101472	0.999688	0.997642	AID
5	4	0.787351	0.040488	0.030528	0.024483	0.933355	0.787351	AID
6	9	0.819304	0.036797	0.032549	0.028433	0.950760	0.819304	AID
7	5	0.842703	0.032950	0.023230	0.028502	0.950913	0.842703	AID
8	8	0.872363	0.872363	0.019369	0.032271	0.964055	0.872363	AID
9	6	0.997159	0.997159	0.043469	0.095310	0.999648	0.997159	AID
MRR								
1	1	0.974346	0.003107	0.001598	0.027060	0.992006	0.974346	AID
2	**18**	**0.996238**	**0.000757**	**0.004100**	**0.021158**	**0.999241**	**0.996238**	**AID**
3	11	0.994517	0.001216	0.003415	0.023088	0.998636	0.994517	AID
4	7	0.968235	0.003091	0.002929	0.025573	0.988577	0.968235	AID
5	15	0.986512	0.001634	0.004652	0.029285	0.996451	0.986512	AID
6	13	0.977519	0.002242	0.003272	0.030718	0.993174	0.977519	AID
7	9	0.994106	0.001177	0.008614	0.068105	0.998540	0.994106	AID
8	12	0.994092	0.001161	0.009081	0.062635	0.998629	0.994092	AID
9	10	0.992901	0.001516	0.006479	0.053474	0.998005	0.992901	AID

Note: N= Neurons, F= Fitness, TE= Training error, VE= Validation error, TE= Testing error, C= Correlation, R-S= R-square, SR= Stop reason AID = All iterations done

Table 4.6: Architecture search for SiO_2-Single Pass

ID	N	F	TE	VE	TE	C	R-S	SR
Surface Roughness								
1	1	0.016492	0.074381	0.041492	0.094811	0.129275	0.016492	AID
2	15	12.52008	0.271154	0.250308	0.301681	0.497682	0.599643	AID
3	**9**	**0.995377**	**0.005061**	**0.060476**	**0.012381**	**0.997687**	**0.995377**	**AID**
4	5	0.574334	0.051339	0.068071	0.044394	0.783732	0.574334	AID
5	12	5.379968	0.174837	0.018664	0.134686	0.307635	0.537865	AID
6	13	0.790775	0.033949	0.168071	0.125832	0.902696	0.790775	AID
7	10	0.969234	0.013100	0.017406	0.078031	0.984737	0.969234	AID
8	11	0.993113	0.006186	0.325791	0.149633	0.996552	0.993113	AID
9	6	0.995695	0.001483	0.018340	0.011342	0.995678	0.988657	AID
MRR								
1	1	0.949016	0.004825	0.007608	0.013993	0.975919	0.949016	AID
2	18	0.115413	0.017326	0.006561	0.015482	0.541852	0.115413	AID
3	11	0.177758	0.023372	0.014597	0.012648	0.170887	0.177758	AID
4	7	0.132705	0.023667	0.021662	0.010353	0.365379	0.132705	AID
5	4	0.995004	0.001335	0.017738	0.011900	0.998972	0.995004	AID
6	**9**	**0.997908**	**0.000813**	**0.021336**	**0.010965**	**0.999647**	**0.997908**	**AID**
7	5	0.996251	0.001140	0.020575	0.010338	0.999314	0.996251	AID
8	8	0.997555	0.000875	0.024212	0.011237	0.999568	0.997555	AID
9	6	0.988691	0.002223	0.018248	0.011262	0.996621	0.988691	AID

Note: N= Neurons, F= Fitness, TE= Training error, VE= Validation error, TE= Testing error, C= Correlation, R-S= R-square, SR= Stop reason AID = All iterations done

Figure 4.5 shows the actual versus predicted values for conventional-single pass by ANN Analysis. The blue line indicates the experimental output and the red line indicates the prediction output (target). The performance of the ANN prediction was evaluated by a regression analysis between the predicted and the experimental values. The ANN prediction yields the statistical coefficient for both of the regression lines are giving the correlation coefficient (R^2) value 0.99 and 0.98 for surface roughness and MRR respectively. The regression coefficients obtained from testing of the ANN were good and within the acceptable limits in both cases. As the correlation coefficient approaches to 1, the accuracy of the prediction improves (Kurt and Kayfeci, 2009). The correlation coefficient range is very close to 1, hence it indicates excellent agreement between the experimental and the ANN predicted results.

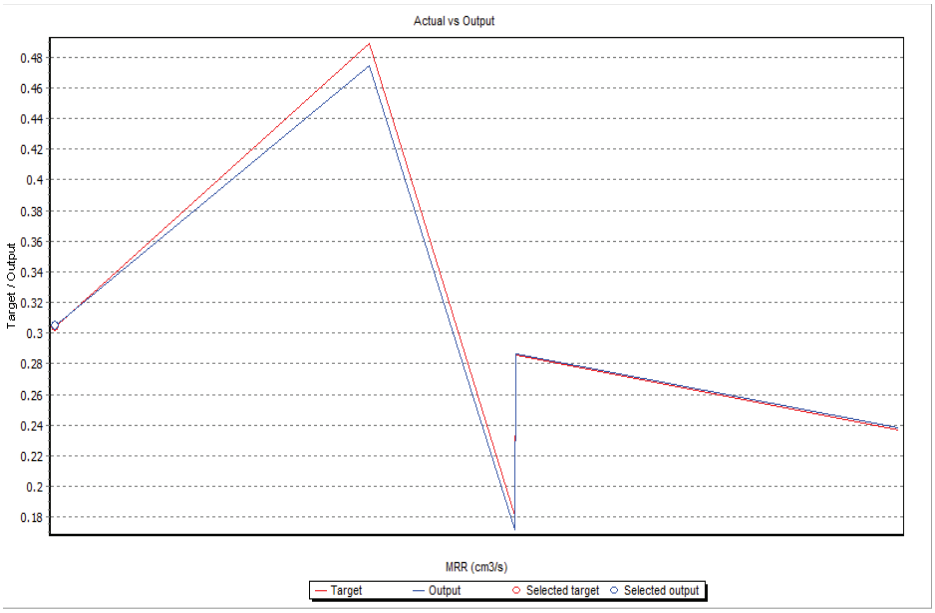

(a) Surface Roughness

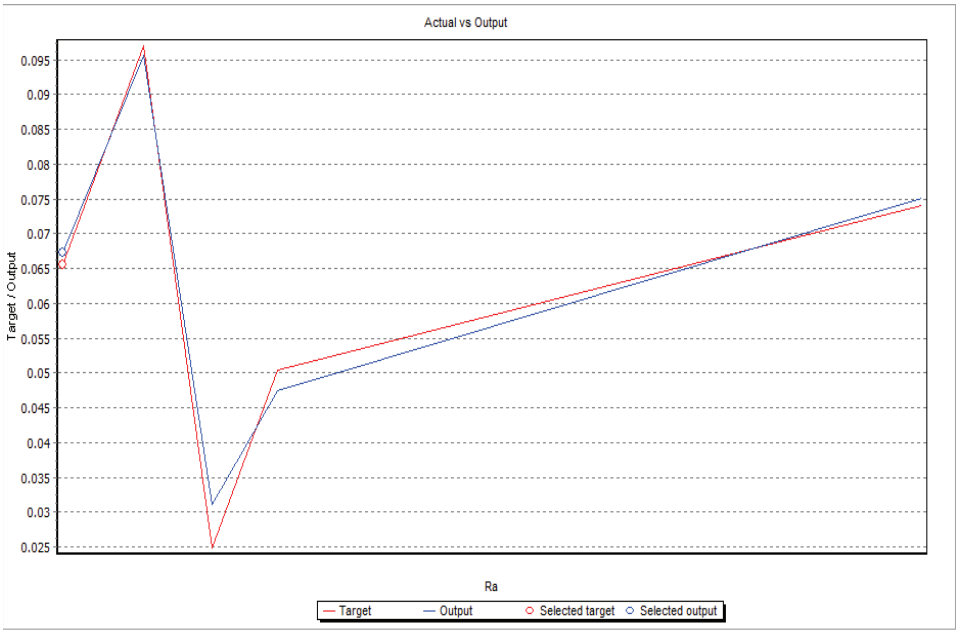

(b) MRR

Figure 4.5: Actual versus predicted values for conventional-single pass

Similarly, Figure 4.6 shows the actual versus predicted values for conventional-single pass by ANN Analysis. The blue line indicates the experimental output and the red line indicates the prediction output (target). The ANN prediction yields the statistical coefficients are giving the correlation coefficient (R^2) value 0.99 for both cases. The regression coefficients obtained from testing of the ANN were perfect and within the acceptable limits in both cases. As the correlation coefficient approaches to 1,

the accuracy of the prediction advances. Thus, the correlation coefficient range is very close to 1. Consequently, it indicates excellent agreement between the experimental and the ANN predicted results. Table 4.7 and Table 4.8 show the range of input and output parameters values for conventional and SiO_2 nanocoolant single pass and multiple pass grinding respectively. Table 4.9 and Table 4.10 are presented for architecture search for conventional coolant and SiO_2 nanocoolant with multiple pass grinding respectively.

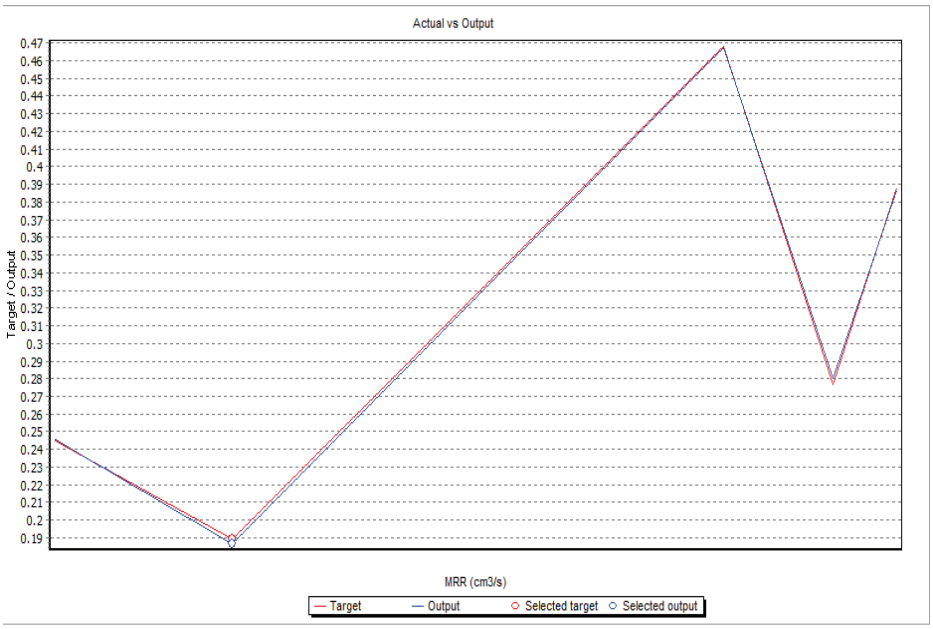

(a) Surface Roughness

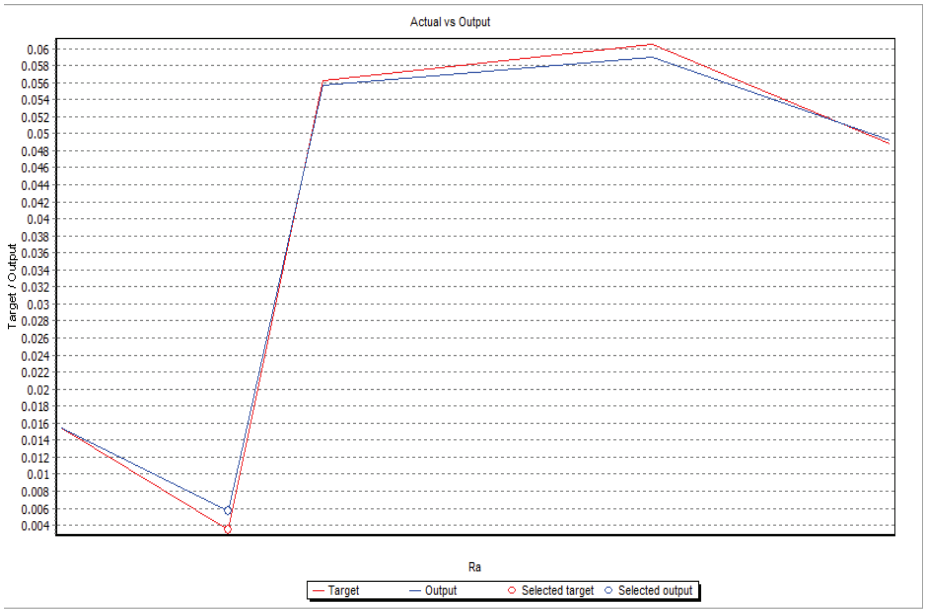

(b) MRR

Figure 4.6: Actual versus predicted values for SiO_2-single pass

Table 4.7: The range of input and output parameters values for single pass grinding

Parameters	Minimum	Maximum
Conventional grinding		
Table Speed (mm/s)	333.33	666.67
Depth of Cut (μm)	0.02	0.06
Surface Roughness (μm)	0.170	0.457
Material Removal Rate (cm^3/s)	0.027	0.152
SiO2 nanocoolant grinding		
Table Speed (mm/s)	333.33	666.67
Depth of Cut (μm)	0.02	0.06
Surafce Roughness (μm)	0.186	0.457
Material Removal Rate (cm^3/s)	0.010	0.058

Table 4.8: The range of input and output parameters values for multiple pass grinding

Parameters	Minimum	Maximum
Conventional coolant		
Table Speed (mm/s)	333.33	666.67
Depth of Cut (μm)	0.02	0.06
Surafce Roughness (μm)	0.187	0.400
Material Removal Rate (cm^3/s)	0.033	0.159
SiO2 nanocoolant		
Table Speed (mm/s)	333.33	666.67
Depth of Cut (μm)	0.02	0.06
Surafce Roughness (μm)	0.2239	0.375
Material Removal Rate (cm^3/s)	0.013	0.112

Figure 4.7 and Figure 4.8 show actual and predicted values for conventional coolant and SiO_2 nanocoolant with multiple pass grinding respectively. The performance of the neural network prediction was evaluated by a regression analysis between the predicted and the experimental values. The regression coefficients obtained from testing of the ANN were perfect and within the acceptable limits in both cases. As the correlation coefficient approaches to 1, the accuracy of the prediction is acceptable. The correlation coefficient range is very close to 1. Thus it indicates excellent agreement between the experimental and the ANN predicted results.

Table 4.9: Architecture search for conventional with multiple pass grinding

ID	N	F	TE	VE	TE	C	R-S	SR
Surface Roughness								
1	1	0.883953	0.022513	0.004986	0.013174	0.986941	0.883953	AID
2	**18**	**0.998321**	**0.002172**	**0.012646**	**0.028586**	**0.999780**	**0.998321**	**AID**
3	11	0.988417	0.007610	0.016988	0.029194	0.998375	0.988417	AID
4	7	0.979744	0.010036	0.013179	0.029276	0.997141	0.979744	AID
5	15	0.989209	0.007556	0.020554	0.030841	0.998260	0.989209	AID
6	13	0.987268	0.008047	0.005581	0.028366	0.997699	0.987268	AID
7	16	0.993438	0.004869	0.009234	0.029381	0.999467	0.993438	AID
8	17	0.989079	0.006394	0.005369	0.035876	0.998707	0.989079	AID
MRR								
1	1	0.991968	0.001431	0.006565	0.023644	0.998313	0.991968	AID
2	**18**	**0.997905**	**0.000689**	**0.005742**	**0.019354**	**0.999538**	**0.997905**	**AID**
3	11	0.997393	0.000797	0.005898	0.020232	0.999374	0.997393	AID
4	7	0.995553	0.001062	0.005858	0.021403	0.998847	0.995553	AID
5	15	0.997747	0.000720	0.002203	0.016833	0.999494	0.997747	AID
6	13	0.996744	0.000884	0.001452	0.016369	0.999219	0.996744	AID
7	16	0.996340	0.000959	0.000725	0.010336	0.999101	0.996340	AID
8	14	0.997379	0.000795	0.002581	0.015343	0.999381	0.997379	AID

Note: N= Neurons, F= Fitness, TE= Training error, VE= Validation error, TE= Testing error, C= Correlation, R-S= R-square, SR= Stop reason AID = All iterations done

Table 4.10: Architecture search for SiO_2 nanocoolant with multiple pass grinding

ID	N	F	TE	VE	TE	C	R-S	SR
Surface Roughness								
1	1	0.952358	0.008931	0.018053	0.037088	0.984222	0.952358	AID
2	**18**	**0.995183**	**0.002422**	**0.024921**	**0.031183**	**0.999099**	**0.995183**	**AID**
3	11	0.984284	0.005360	0.016197	0.013763	0.996549	0.984284	AID
4	7	0.982542	0.005600	0.020976	0.022371	0.996423	0.982542	AID
5	15	0.990264	0.003976	0.020695	0.024468	0.998350	0.990264	AID
6	13	0.990996	0.003833	0.022881	0.017140	0.998422	0.990996	AID
7	14	0.989989	0.004026	0.009807	0.025953	0.998105	0.989989	AID
8	12	0.988438	0.004399	0.007814	0.011753	0.998019	0.988438	AID
MRR								
1	1	-0.315868	0.028451	0.006431	0.028397	0.160204	0.315868	AID
2	18	0.628088	0.014661	0.005098	0.042006	0.913600	0.628088	AID
3	11	0.790516	0.011528	0.003650	0.055038	0.971231	0.790516	AID
4	**7**	**0.966930**	**0.004116**	**0.010974**	**0.073012**	**0.992002**	**0.966930**	**AID**
5	4	0.434784	0.019056	0.011107	0.048682	0.849345	0.434784	AID
6	9	0.897173	0.008106	0.008975	0.066582	0.983870	0.897173	AID
7	5	0.307026	0.020752	0.005979	0.043788	0.739724	0.307026	AID
8	8	0.460940	0.019919	0.008800	0.042534	0.828332	0.460940	AID
9	6	-0.51821	0.032062	0.009124	0.023176	0.551642	-0.51821	AID

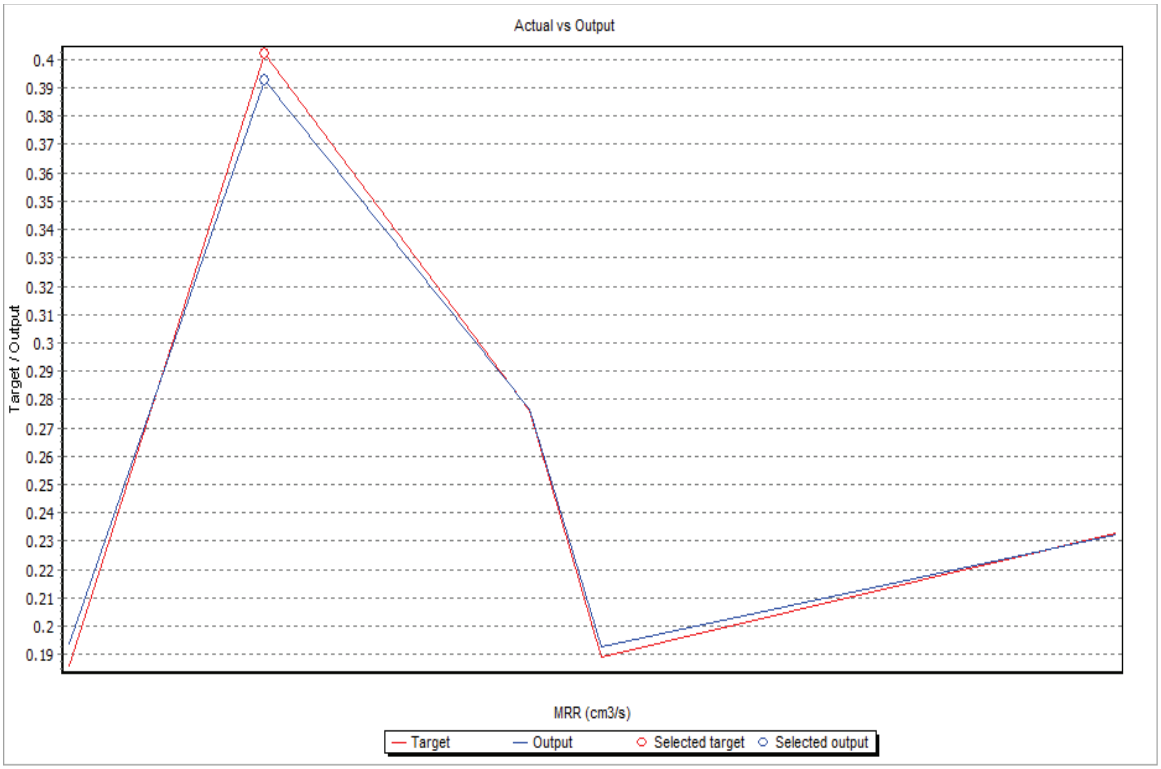

(a) Surface Roughness

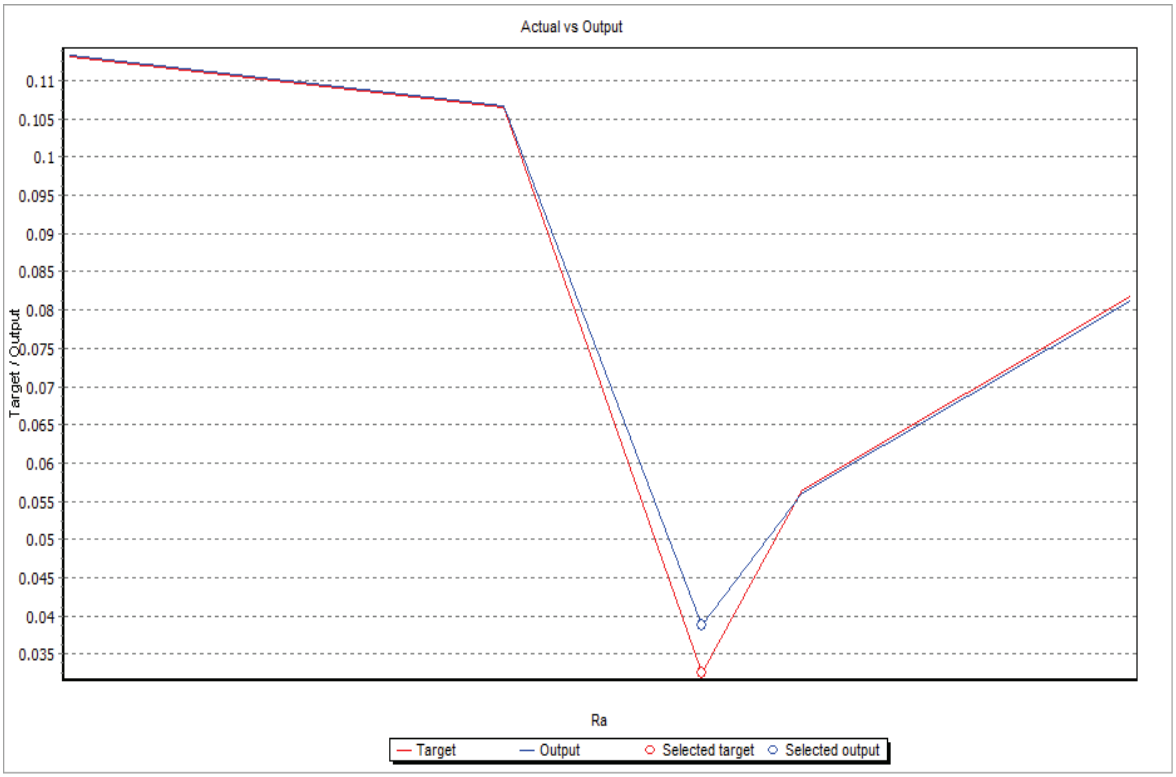

(b) MRR

(c)

Figure 4.7: Actual versus predicted values for conventional-Multiple Pass

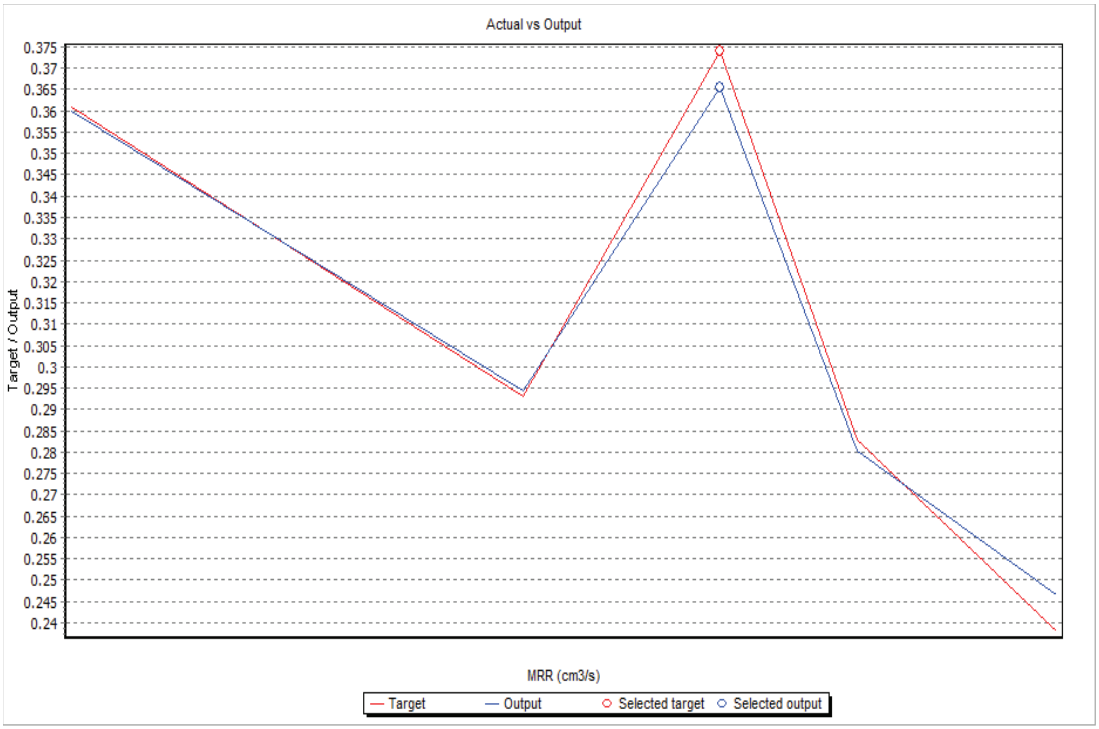

(a) Surface Roughness

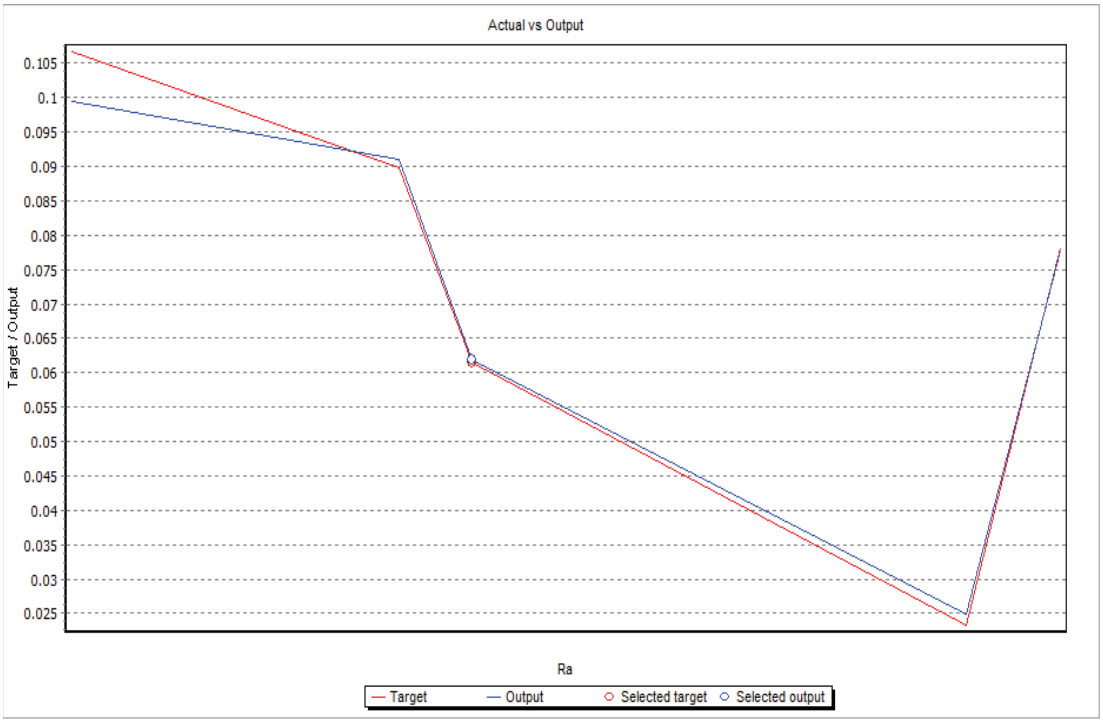

(b) MRR

Figure 4.8: Actual versus predicted values for SiO_2-Multiple Pass

4.4 OPTIMIZATION

From the experimental and analysis results for single pass conventional grinding, the minimum surface roughness and maximum MRR was chosen from all of the data. From the data, two values of the lowest surface roughness were carried out from each of the analysis since surface roughness is most prior than MRR which is 0.204 and 0.250 for 1st order of RSM, 0.186 and 0.247 for 2nd order of RSM, and also 0.237 and 0.317 for RBF. Between the two values of the surface roughness, one with higher MRR value was choose. So, we can conclude that the table speed 666.67mm/s with 0.02 µm depth of cut are the most optimize value that can be used for the single pass conventional grinding. Comparison between the RSM model and ANN for conventional coolant and SiO2 nanocoolant are presented in Table 4.11 and Table 4.12 respectively.

Table 4.11: Comparison between RSM model and ANN for conventional coolant

Table Speed (mm/s)	Depth of Cut (µm)	Surface Roughness				MRR			
		Exp.	RSM		RBF	Exp.	RSM		RBF
			1st order	2nd order			1st order	2nd order	
Single pass grinding									
666.67	0.02	0.151	0.156	0.170	0.164	0.046	0.044	0.046	0.031
666.67	0.04	0.181	0.184	0.174	0.172	0.097	0.097	0.101	0.043
Multiple pass grinding									
666.67	0.02	0.186	0.168	0.187	0.194	0.063	0.063	0.064	0.055
666.67	0.04	0.189	0.190	0.191	0.193	0.113	0.110	0.115	0.110

4.5 MICROSTRUCTURE ANALYSIS

Figure 4.9 shows the microstructure result of surface workpiece between conventional and SiO_2 grinding. The microstructure was magnified using the 200x and 700x magnifier of the microscope. From the figure, it can be observed that there are crack, peak, and valley, cavity, grinding marks and also flat surface on of the surface workpiece. In order to get the best quality surface of the workpiece, dressing plays the important role. The cracks usually happen when the dressing are not doing very well on

the grinding wheel. From the figure, it can be concluded that grinding with SiO_2 gives the better surface workpiece compare to the conventional grinding. This is due to the SiO_2 nanoparticles properties itself. The smaller the size of the particles, the better surface finishes.

Table 4.12: Comparison between RSM model and ANN for silicon oxide nanocoolant

Table Speed (mm/s)	Depth of Cut (µm)	Surface Roughness				MRR			
		Exp.	RSM 1st order	RSM 2nd order	RBF	Exp.	RSM 1st order	RSM 2nd order	RBF
Single pass grinding									
666.67	0.02	0.189	0.204	0.186	0.237	0.015	0.004	0.010	0.018
666.67	0.04	0.245	0.250	0.247	0.317	0.003	0.026	0.013	0.006
Multiple pass grinding									
666.67	0.02	0.238	0.251	0.240	0.246	0.107	0.103	0.112	0.099
666.67	0.04	0.283	0.280	0.278	0.283	0.090	0.076	0.089	0.091

Magnified	Conventional	SiO_2
200x	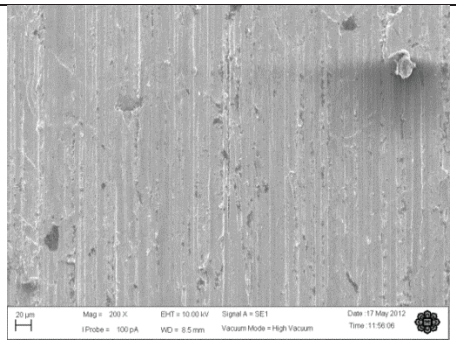	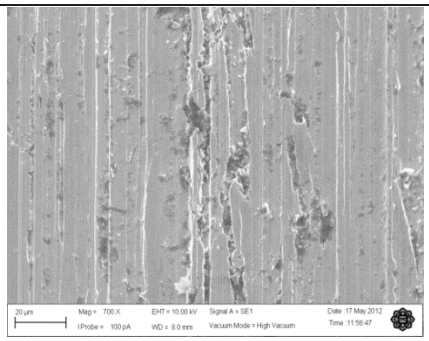
700x	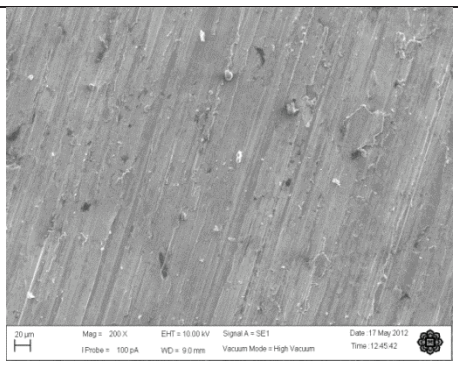	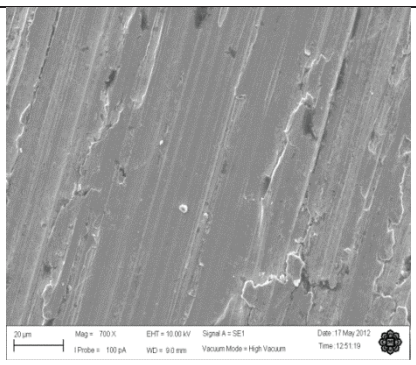

Figure 4.9: Microstructure of surface workpiece of conventional and nanocoolant grinding

CHAPTER 5

CONCLUSIONS AND RECOMMENDATIONS

5.1 CONCLUSIONS

The objectives of this project are to investigate the performance of grinding of ductile cast iron based on Response Surface Method (RSM), to develop optimization model for grinding parameters using a Radial Basis Function (RBF) technique and also to investigate the effect of water based SiO_2 nanoparticles to the precision surface grinding.

As the overall experimental and analysis had done, it can be simplify that all of the objectives for this project are achieved. In order to optimize the two parameters to yield the minimum surface roughness and the maximum material removal rate value in the process, a combination of knowledge in variable table speed and depth of cut parameters is very crucial. The use of Response Surface Methodology is very useful in analyzing the effect and the interaction of the factors affecting the surface texture of the workpiece. The graphs analysis clearly shows that the parameter used which is table speed and depth of cut was positively correlated with the surface roughness and MRR. The correlation of determination R^2 also gives the 0.98 value for almost parameters which is just gives 0.02 errors. The SiO_2 multiple pass grinding gives the best value of percentage error between the RSM and experimental value is 0.4%.

For Artificial Neural Network (ANN) which using Radial Basis Function (RBF), it can be conclude that the uncertainty analysis using ANN will yield the results approximate with the analytical method. This technique or approve method can be used to determine problem solution of uncertainty propagation. This not only for this project but other equation also can be used to determine the problem of uncertainty. The correlation of determination R^2 for each parameter also gives the 0.99 value which is just gives 0.01 errors. The SiO_2 multiple pass grinding gives the best value of percentage error between the RBF and the experimental value is 0.3%.

The third objectives of the project also achieved which to investigate the effect of water based SiO_2 nanoparticles to the precision surface grinding. Grinding process with SiO_2 nanocoolant gives the better result of the surface roughness and surface finish compare to the conventional grinding.

5.2 RECOMMENDATIONS

The recommendation has been drawn based on present study, which is presented as follows:

i) Use the different concentration of nanofluids to investigate the effect on surface roughness and MRR.

ii) Use another optimization method such as Fuzzy Logic, PSO and SVM.

iii) Increase the design level so that the output parameters will be more accurate.

REFERENCES

Abraham, A. 2005. Artificial neural network. *Handbook of measuring system design*. **129**: 900-906.

Baseri, H., Razaei, S.M., Rahimi, A., and Saadat, M. 2008. Analysis of the disc dressing effects on grinding performance PART I: Simulation of the disc dressed wheel surface. *Mach. Sc. And Tech.* **12**(2): 197-213.

Box, G.E.P. and Draper, N.R. 1987. Empirical model-building and response surfaces. New York: Jon Wiley & Sons.

Bradley, N. 2007. The response surface methodology. Indiana University of South Bend, USA.

Cakir, O., Yardimeden, A., Ozben,T. and Kilikcap, E. 2007. Selection of Cutting Fluids in Machining Process. *Journal of Achievements in Materials and Manufacturing Engineering*. **25**(2): 99-100.

Comley, P., Walton, I., Jin, T. and Stephenson, D.J. 2006. A High Removal Rate Grinding Process for the Production of Automotive Crankshafts. *Cranfield Precision Division of Cinetic Landis Grinding Systems Ltd*. **55**: 1-2

Ding, Y., Chen, H., Wang, L., Yang, C. Y., He, Y., Yang, W., Lee, W. P., Zhang, L. and Huo, R. 2007. *Heat Transfer Intensification Using Nanofluids*. **25**: 23-25.

Ding, Z.W., Cheah, S.C., and Saeid, N.H. 2009. Parametric Study of Heat Transfer Enhancement using Nanofluids, *Proceedings of ICEE 2009 3rd International Conference on Energy and Environment*. pp. 1-11.

Fristak,V., Remenarova, L. and Lesny, J. 2012. Response surface methodology as optimization tool instudy of competitive effect of Ca^{2+} and Mg^{2+} ions in sorption Process of Co^{2+} by dried activated sludge. *Journal of Microbiology, Biotechnology and Food Sciences*. **1**(5): 1235-1249.

Ghafari, S., Aziz, A. H., Isa, H. M. and Zinatizadeh, A. A. 2009. Application of response surface methodolgy (RSM) to optimize coagulation-flocculation treatment of leachate using poly-aluminum chloride (PAC) and alum. *Journal of Hazardous Materials*. **163**: 650-656.

Goldstein, R.J., Joseph, D.D. and Pui, D.H. 2000. Convective Heat Transport in Nanofluids. *Enhancing Thermal Conductivity of Fluids With Nanoparticles, Development and Applications of Non-Newtonian Flows*, FED-Vol.231/MD ASME, New York. **66**: 99-105.

Helmi, H. M., Azuddin, M. and Abdullah, W. 2010. Investigation of Surface Roughness and Material Removal Rate (MRR) on Tool Steel Using Brass and Copper Electrode for Electrical Discharge Grinding (EDG) Process. *International Journal of Integrated Engineering* (Issue on Mechanical, Materials and Manufacturing Engineer).

Hou, Z. B. and Komanduri, R. 2003. On the mechanics of the grinding process, Part II thermal analysis of fine grinding. *International Journal of Machine Tools & Manufacture*. **44**(2004): 247-270.

Jackson, M.J. 2010. Numerical analysis of small recessed silicon carbide grinding wheels. *Journal of Achievements in Materials and Manufacturing Engineering*. **43**(1): 27-29.

Jahirul, M. I., Saidur, R. and Masjuki, H. H. 2009. Application of artificial neural network to predict brake specific fuel consumption of retrofitted CNG engine. *International Journal of Mechanical and Material Engineering*. **4**(3): 249-255.

Kalpakjian, S., 1995. Manufacturing engineering and technology, 3rd ed. NY: Addison-Wesley.

Kalpakjian, S., and Schmid, S.R. 2001. Manufacturing processes for engineering materials, 4th ed. USA: Pearson Education Inc.

Kamely, A. M., Kamil, M. S. and Chong, W. C. 2011. Mathematical modeling of surface roughness in surface grinding operation. *Journal of World Academy of Science, Engineering and Technology*. **80**:1-4.

Kheram, M.A. 2008. Numerical study on convective heat transfer for water-based alumina nanofluid. *International Journal of Nano Dimension*. **1**(4): 297-304.

Krajnik, P., Kopac, J. and Sluga, A. 2005. Design of Grinding Factors Based on Response Surface Methodology. *Journal of Materials Processing Technology* **162-163**: 629-636.

Kurt, H., and Kayfeci, M., 2009. Prediction of thermal conductivity of ethylene glycol-water solutions by using artificial neural network. *Applied Energy*. **86**: 2244-2248.

Lenth, V. S., 2009. Response-surface methods in R, using RSM. *Journal of Statistical Software*. **32**(7): 2-17.

Liao, Y.S., Luo, S.Y. and Yang, T.H. 1998. A Thermal model of the wet grinding process. *Journal of Materials Processing Technology*. **101**(1998): 137-145.

Malkin, S. 1984. *Grinding of metals: theory and application*, American Society for Metals. **3**(2): 95-97.

Malkin, S., and Anderson, R. B., 1974, Thermal aspects of grinding, Part 1 - Energy partition, *ASME Journal of Engineering for Industry*, **96**:1177-1183.

Malkin, S. and Guo, C. 2007. Thermal analysis of grinding. **56**: 760-761.

McCulloch, W.S., and Pitts, W.H., 1943. A Logical Calculus of the Ideas Immanent in Nervous Activity. *Bulletin of Mathematical Biophysics.* **5**: 115-133.

Middle, J. E. 2005. Grinding equivalent and grinding ratio as parameters for grinding wheel wear. *The Production Engineer*.

Myers, R.H., and Montgomery, D.C., 2002. Response surface methodology: process and product optimization using design experiment, A Wiley-Interscience Publication.

Newman, S.T., and Ho, K.H., 2004. State of the art electrical discharge machining (EDM), *Int. J. Mach. Tools Manuf*. **43**, 1287–1300.

Park, J., and Sandberg, J.W., 1991. Universal approximation using radial basis functions network, *Neural Computation*, **3**: 246-257.

Rumelhart, D. and McClelland, J. 1986. Parallel Distributed Processing. MIT Press, Cambridge, Mass.

Samhouri, M.S and Surgenor, B.W. 2005. Surface roughness in grinding: on-line prediction with adaptive neuro-fuzzy inference system. **33**: 57-59.

Sampaio, C. F., Faveri, D. D., Mantovani, C. H., Passos, L. M. F., Perego, P. and Converti, A. 2006. Use of response surface methodology for optimization of xylitol production by the new yeast strain. *Journal of Food Engineering*. **76**: 376-386.

Saterlie, M., Sahin, H., Kavlicoglu, B., Liu, Y. and Graeve, O. 2011. *Particle Size Effects in the Thermal Conductivity Enhancement of Copper-based Nanofluids*.

Senussi, G.H. 2007. Interaction effect of feed rate and cutting speed in CNC- turning on chip micro-hardness of 304-austenitic stainless steel. *Journal of World Academy of Science, Engineering and Technology*. Volume **28**: 121-123.

Shen, B. 2008. Minimum quantity lubrications grinding using nanofluids.

Todd, R.H., Allen, D.K., and Alting, L., 1994. Manufacturing processes reference guide, Industrial Press Inc.

Tou, J.T., and Gonzalez, R.C., 1974. Pattern recognition, MA: Addison-Wesley.

Wang, X.Q., Mujumdar and Arun, S. 2006. Heat Transfer Characteristics of Nanofluids: A Review. *International Journal of Thermal Sciences*. **46**(2007): 1-9.

Wang, X. Q., Mujumdar and Arun, S. 2008. A Review on Nanofluids- Part II: Experiments and Application. *Brazilian Journal of Chemical Engineering*. **25**(04): 631-648.

Zhu, H., Wu, D., Wang, L. and Liu, L. 2009.*Critical issues in nanofluidspreparation, characterization and thermal conductivity*. *Current Nanoscience.* **5**: 103-112.